NUCLEOLAR REORGANIZATION AFTER CELLULAR STRESS IS ORCHESTRATED BY SMN SHUTTLING BETWEEN NUCLEAR COMPARTMENTS

Shaqraa Musawi[1,2,†], Lise-Marie-Donnio[1,†,*], Zehui Zhao[1], Charlène Magnani[1], Olivier Binda[1,3], Jianbo Huang[1], Phoebe Rassinoux[1], Arnaud Jacquier[1], Laurent Coudert[1], Patrick Lomonte[1], Cécile Martinat[4], Laurent Schaeffer[1], Jocelyn Côté[3], Pierre-Olivier Mari[1] and Giuseppina GIGLIA-MARI[1,*]

1. Institut NeuroMyoGène-Pathophysiology and genetics of neuron and muscle (INMG_PGNM), CNRS UMR 5261, INSERM U1310, Université de Lyon, Université Claude Bernard Lyon 1, Lyon, France
2. Department of Medical Laboratories Technology, College of Applied Medical Sciences, Jazan University, Jazan, Saudi Arabia.
3. University of Ottawa, Faculty of Medicine, Department of Cellular and Molecular Medicine, K1H 8M5, Ottawa, Ontario, CANADA
4. INSERM/UEPS UMR 861, Paris Saclay Université, I-STEM, 91100 Corbeil-Essonnes, France

† These authors contributed equally to this work

* Co-Corresponding authors

Keywords:

SMA, SMN, RNAP1, DNA repair, UV lesions, Nucleolus, Coilin, Fibrillarin

ABSTRACT

SMA is an autosomal recessive neuromuscular disease caused by mutations in the multifunctional protein SMN. Within the nucleus, SMN localizes to Cajal bodies (CBs), which have been shown to be associated with nucleoli, nuclear organelles dedicated to the first steps of ribosome biogenesis. The highly organized structure of the nucleolus can be dynamically altered by genotoxic agents. After genotoxic stress, RNAP1, Fibrillarin (FBL) and nucleolar DNA are exported to the periphery of the nucleolus and once DNA repair is fully completed the organization of the nucleolus is restored. We found that SMN is required for the restoration of the nucleolar structure after genotoxic stress. Unexpectedly, during DNA repair, SMN shuttles from the CBs to the nucleolus. This shuttling is important for nucleolar homeostasis and relies on the presence of Coilin and the activity of PRMT1.

32 ## INTRODUCTION

33 The nucleolus is a nuclear membrane-less organelle with a very structured internal
34 organization, which associates with its different functions in ribosomal biogenesis: transcription
35 of ribosomal DNA (rDNA) and early ribosomal RNA (rRNA) maturation [1]. Nucleoli are formed
36 around the rDNAs which are composed of tandem head-to-tail repeats and their structure is
37 thought to be strictly dependent on the transcriptional activity of the RNA polymerase I (RNAP1)
38 [2]. Despite a very structured organization, nucleoli are very dynamic organelles, their shape and
39 number can vary through the cell cycle and many proteins can enter or exit the nucleolus
40 depending on physiological processes or cellular stress responses. This organized structure can
41 be dynamically altered by both genotoxic agents and general cellular stress [3]. For instance, drugs
42 that alter RNAP1 transcription (i.e. cordycepin, actinomycin D, etc.) may cause nucleolar
43 segregation at the periphery of the nucleolus into structures known as nucleolar caps.
44 Furthermore, drugs that block rRNA processing or the topoisomerase II (i.e. doxorubicin) but do
45 not interfere with RNAP1 transcription induce a disruption of the compact nucleolar environment
46 and nucleolar necklaces appear [4].

47 Amongst different cellular stresses known to modify the nucleolar organization, UV-
48 irradiation has the benefit of being a quick, punctual, and chemically clean method. Moreover,
49 cells are able to repair UV-induced lesions and hence reverse their stress status. UV-induced DNA
50 lesions are repaired by the Nucleotide Excision Repair system (NER)[5]. NER also repairs DNA helix-
51 distorting adducts, including environmental pollutants, the oxidative-damage derived
52 cyclopurines [6] and participates in the repair of the ROS-induced oxidized guanine (8-oxoG) [7].

53 During UV-irradiation, it has been shown that the nucleolus is not fully disrupted but
54 nucleolar proteins (RNAP1, Fibrillarin [FBL]) and nucleolar DNA are exported to the periphery (for
55 simplicity this phase will be called "displacement") of the nucleolus and when DNA repair is fully
56 completed the proper nucleolar structure is restored (for simplicity this phase will be called
57 "repositioning")[8]. Using a best-candidate approach, we recently found that structural proteins
58 like Nuclear Myosin I (NMI) and **β**-Actin (ActB) seem to play a prominent role in this process [9]. In
59 cells depleted from NMI and ActB, nucleolar structure is not restored and both nucleolar proteins
60 and nucleolar DNA remain at the periphery of the nucleolus, although DNA repair is completed

61 and transcription is resumed [9]. However, the exact mechanism of NMI and ActB actions on
62 nucleolar reorganization has not yet been elucidated, probably because many other molecular
63 actors are still unknown. In order to find a complete molecular mechanism, several structural and
64 nucleolar proteins have been scrutinized and a certain number have been found to be crucial to
65 restore a proper nucleolar structure after DNA repair completion. One of these proteins is FBL.
66 Consequently, we studied whether FBL interacting partners were also involved in this process.
67 Amongst these different FBL partners, we investigated whether the protein Survival of Motor
68 Neurons (SMN) was implicated in the restoration of the nucleolar structure after DNA repair
69 completion.

70 Spinal Muscular Atrophy (SMA) is an autosomal recessive neuromuscular disease, which
71 affects neurons that controls the voluntary movement of muscles (motoneurons) [10]. In SMA,
72 motoneurons are progressively lost leading to progressive muscle wasting and atrophy because
73 muscles no longer receive signals from the motor neurons of the spinal cord. Children affected
74 with SMA have symptoms that can vary greatly depending on the age of disease onset and its
75 severity. Normal activities, such as crawling, walking, maintaining a seated position, controlling
76 head movements, breathing and swallowing might be affected [10]. With an incidence of 1 in 6,000-
77 10,000 live births, SMA is the most prevalent hereditary cause of infant mortality [11].

78 SMA is caused by bi-allelic mutations in the *SMN1* gene (Survival of Motor Neuron: SMN)
79 and the disease phenotype is modified by the number of copies of a second paralog gene,
80 *SMN2*, which is always present in SMA patients [12]. *SMN1* produces a full-length functional version
81 of the SMN protein whereas in *SMN2*, the absence of exon 7 in most of the transcripts produces
82 an unstable version of the SMN protein (SMNΔ7). *SMN2* can express about 10-15% of the full-
83 length protein, which is insufficient to avoid the disease.

84 SMN is a multifunctional ubiquitous protein involved in many cellular processes, such as
85 biogenesis and trafficking of ribonucleoproteins, local translation of messenger RNAs, etc [13]. SMN
86 protein is ubiquitously expressed and is localized to both the cytoplasm and the nucleus. Within
87 the nucleus, SMN localizes in Gems and Cajal bodies (CBs), which have been shown to associate
88 with nucleoli [14]. Within CBs, SMN interacts with the protein Coilin [15]. Interestingly, in certain

89 conditions, SMN is also detected in the nucleoli of mammalian primary neurons and colocalized
90 with FBL [16]. In addition, a transient colocalization of SMN at the periphery of nucleoli with FBL
91 after actinomycin D treatment in 10–20% of Hela cells [17,18] suggests that SMN could be present
92 in the nucleolus under stress conditions. SMN Tudor domain is involved in the binding to RGG
93 motifs containing proteins such as FBL and Coilin [19].

94 We investigated the possible role of SMN in nucleolar reorganization during both
95 displacement and repositioning of RNAP1, during and after DNA repair of UV-induced damage
96 and generally after stress induction. We show here that in the absence of a functional SMN, both
97 RNAP1 and FBL remain at the periphery of the nucleolus after DNA repair completion even once
98 transcription is fully restored. Interestingly, we could reveal that SMN (and its complex) shuttles
99 to the nucleolus after DNA repair completion. We determine that this shuttling is dependent on
100 the presence of Coilin and governed by PRMT1-dependent arginine methylation activity.
101 Additionally, we disclosed that the presence of FBL is important for the proper restoration of
102 SMN into CBs. Importantly, we could show that SMN cells show a sensitivity to DNA damage and
103 in particular, to chronic oxidative damage. Our results open up new avenues of research on the
104 SMN function in nucleolar homeostasis and its impact on SMA pathology.
105

106 ## RESULTS

107 **RNAP1 and FBL repositioning after DNA repair completion are SMN-dependent.**

108 To investigate a possible role of SMN in nucleolar reorganization in response to cellular
109 stress, we investigated whether the previously reported [8] RNAP1 UV-induced displacement and
110 the later repositioning were still happening in the absence of SMN. As SMN-deficient cells we
111 used primary fibroblasts from SMA patients (Figure S1A), SMA iPSC-derived motoneurons (Figure
112 S2) and transformed fibroblasts in which SMN was downregulated by lentiviral transfection of 2
113 independent inducible shRNAs against SMN 3'UTR (Figure 1A). Using these cell lines, we
114 performed immunofluorescent (IF) assays to detect both RNAP1 and FBL positioning in the
115 absence of damage (No UV), 3 hours post-UV-irradiation (PUVI) (this time point corresponds to
116 the minimum of RNAP1 transcriptional activity as found in [8] and at 40 hours PUVI (this time point
117 corresponds to the RNAP1 full recovery of transcriptional activity and full DNA repair as described
118 in [8]). Wild-type fibroblasts, SV40-transformed MRC5 and primary C5RO were used as positive
119 controls, while Cockayne Syndrome type B (CSB) TC-NER deficient fibroblasts (both transformed
120 and primary; termed CS1AN) were used as negative control, as used in [8]. For iPSC-derived
121 motoneurons, WT and SMA iPSC-derived neuronal progenitors were differentiated into
122 motoneurons [20].

123 As described in [8], UV-irradiation induced a displacement of both RNAP1 and FBL to the
124 periphery of nucleoli in all cell lines tested (Figures 1B and 1C, Figures S1B and S1C, Figure 2 at
125 3h PUVI). As expected, in wild-type cells (MRC5, shSCRAMBLE and C5RO) both RNAP1 and FBL
126 recovered their position within the nucleoli at 40 hours PUVI (Figures 1B and 1 C, Figures S1B
127 and S1C). In contrast, in cells depleted of SMN (Figures 1B and 1 C, Sh5-SMN and Sh6-SMN),
128 primary fibroblasts mutated in *SMN1* (Figures S1B and S1C, SMA1) and SMA iPSC-derived
129 motoneurons (Figures S2A and S2B) neither RNAP1 nor FBL recovered the proper position within
130 the nucleoli after DNA repair completion. As previously demonstrated [8], in CSB-deficient cells no
131 return of the RNAP1 and FBL was observed (Figures 1B and 1C, CS1AN-SV) (Figures S1B and
132 S1C, CS1AN).

133 In CSB-deficient cells, the repositioning of RNAP1 and FBL is impeded because DNA
134 lesions on the transcribed strand of rDNA genes are not properly repaired and RNAP1

135 transcription is not restored [8]. To investigate whether this was the case in SMN-deficient cells, we
136 performed an RNA-fish assay detecting the pre-rRNA transcript using a specific probe against
137 the 47S product (Figure S3A) and could determine (Figures S3B and S1E) and quantify (Figures
138 1D and S1D) that RNAP1 transcription is restored in SMN-deficient cells at 40 hours PUVI as in
139 wild-type cells. In parallel, the involvement of SMN in Nucleotide Excision Repair (NER) was
140 studied by performing UDS (Figure S4A), RRS (Figure S4B) and TCR-UDS (Figures S4C and S4D)
141 experiments in cells depleted of SMN. Our results clearly show that SMN has no role in NER
142 (Figure S4).

143 Taken together, these results indicate that in the absence of SMN, RNAP1 and FBL are
144 correctly displaced at the periphery of the nucleolus in response to DNA damage but are not
145 repositioned within the nucleolus once DNA repair reactions are completed and RNAP1
146 transcription is restored.

147

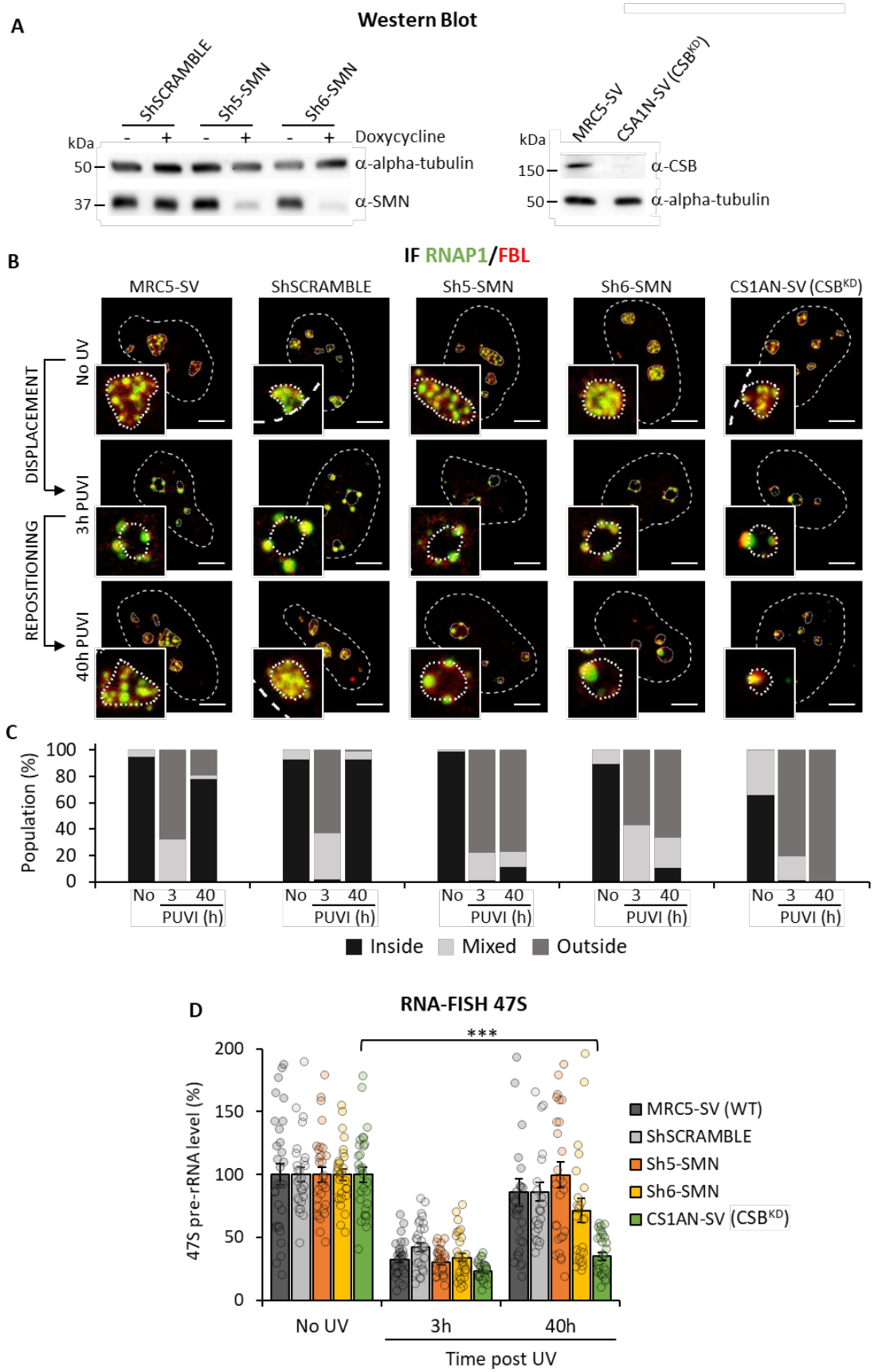
A
Western Blot
ShSCRAMBLE
Sh5-SMN
Sh6-SMN
Doxycycline
kDa
50
37
α-alpha-tubulin
α-SMN
MRC5-SV
CSA1N-SV (CSB^KD)
150
α-CSB
B
IF RNAP1/FBL
MRC5-SV
ShSCRAMBLE
Sh5-SMN
Sh6-SMN
CS1AN-SV (CSB^KD)
DISPLACEMENT
REPOSITIONING
No UV
3h PUVI
40h PUVI
C
Population (%)
100
80
60
40
20
0
No 3 40
PUVI (h)
Inside
Mixed
Outside
D
RNA-FISH 47S
***
47S pre-rRNA level (%)
200
150
100
50
0
No UV
3h
40h
Time post UV
MRC5-SV (WT)
ShSCRAMBLE
Sh5-SMN
Sh6-SMN
CS1AN-SV (CSB^KD)

148

149 **Figure 1: RNAP1 and FBL localization during DNA repair in SMN deficient transformed**
150 **fibroblasts.**
151 ***(A)*** *Western Blot of SMN and CSB on whole cell extracts of transformed fibroblasts (MRC5-SV*
152 *cells). Doxycycline treatment induces the expression of the ShRNA against SMN.* ***(B)***
153 *Representative confocal microscopy images of immunofluorescence (IF) assay against RNAP1*
154 *(green) and FBL (red) in transformed fibroblasts, at different times PUVI. Nuclei and nucleoli are*
155 *indicated by dashed lines and dotted lines respectively. Scale bar: 5µm* ***(C)*** *Quantification of cell*
156 *number for RNAP1 localization (inside the nucleolus, outside the nucleolus or mixed localization)*
157 *at different times PUVI.* ***(D)*** *Quantification of RNA-FISH assay showing the 47S pre-rRNA level*
158 *after UV-C exposure in transformed fibroblasts. Error bars represent the SEM obtained from at*
159 *least 27 cells. P-value of student's test compared to No UV condition: ***<0.001*
160
161
162 **SMN-complex shuttles in the nucleolus and co-localizes with nucleolar proteins after UV**
163 **irradiation.**
164 We showed that SMN is required for the proper repositioning of RNAP1 and FBL at late
165 time points PUVI. We questioned how SMN could be involved in this mechanism if, usually, it is
166 not present in the nucleoli. In fact, SMN protein is typically located in the cytoplasm and within
167 the nucleus where SMN is found in CBs together with Coilin and in Gems without Coilin. To study
168 the localization of SMN and RNAP1 during the DNA repair process, we initially performed
169 immunofluorescence assays at 3 hours and 40 hours PUVI in wild-type cells. Remarkably, at 40h
170 PUVI, two co-existing populations of cells could be detected: (i) a majority of cells in which RNAP1
171 is repositioned within the nucleolus and SMN is localized in the CBs/Gems and (ii) a minority of
172 cells in which RNAP1 is still localized at the periphery of the nucleolus and SMN is unusually
173 localized at the periphery of the nucleolus and cannot be detected in CBs/Gems anymore
174 (Figures S5A, S5B, S5C). Because of this result, we decided to extend our analysis by adding a
175 time point intermediate between 3h and 40h PUVI (24 h PUVI) and a time point beyond the 40h
176 PUVI (48h PUVI) and performed the IF assays against SMN and different nucleolar proteins or
177 SMN protein partners (Figure 2). Importantly, we verified the RNAP1 transcriptional activity by

178 RNA-FISH of 47S at 24h and 48h PUVI and show that RNAP1 transcription is not yet restored at
179 24h PUVI but it's fully recovered at 48h PUVI (Figure S5D). Surprisingly, at 24h PUVI, our results
180 revealed the presence of SMN at the periphery of and/or within the nucleolus in the vast majority
181 of cells (Figure 2A, quantification in 2D). Concomitantly, at 24h PUVI, RNAP1 was found to be
182 localized at the periphery of the nucleolus (Figure 2A, quantification in 2E). On the other hand,
183 we observed a complete return to the undamaged condition (RNAP1 within the nucleolus and
184 SMN in the CBs) at 48h PUVI in the vast majority of cells (Figure 2A, quantification in 2D and 2E).
185 Despite the presence of SMN and RNAP1 at the nucleolar periphery together at 24 h post-UV,
186 no co-localization between these two proteins was observed (Figure 2A, panel 24h PUVI).

187 We showed that the loss of SMN alters FBL localization at 40 h PUVI (Figures 1B and S1B).
188 Using GST pull-down assays we confirmed that FBL from cell extracts interacts with SMN [17,21,22]
189 (Figure S5E). Furthermore, using a panel of SMA-linked TUDOR domain mutants, we established
190 that FBL-SMN interactions require an intact TUDOR domain (Figures S5E and S5F). We, therefore,
191 examined the localization of SMN and FBL during the DNA repair process (Figure 2B,
192 quantification in 2F). Interestingly, we observed a substantial co-localization between SMN and
193 FBL at 24 h PUVI within the nucleolus (Figure 2B, panel 24h PUVI). The co-localization can also
194 be observed at 40 h PUVI in the population of cells that, at this time point, have not yet restored
195 the FBL position within the nucleolus (Figure S5B).

196 In the absence of damage, SMN co-localizes and interacts with Coilin in CBs [15], however
197 after DNA damage induction, it has been shown that CBs are disrupted [23]. Because of this
198 evidence, we examined the localization of Coilin and its interactions with SMN during the DNA
199 repair process. Interestingly, Coilin is localized to the periphery of the nucleolus already at 3h
200 PUVI (Figure 2C, panel 3h PUVI) and remains in this location at 24h PUVI (Figure 2C, panel 24h
201 PUVI) and at 40h PUVI (Figure 2C, panel 40h PUVI) in the subset of cells that did not yet reposition
202 RNAP1. Remarkably, when Coilin is at the periphery of the nucleolus, no colocalization with SMN
203 is observed (Figure 2C).

204 To investigate whether the shuttling of SMN within the nucleolus is specific to UV damage
205 or also happening when cells are submitted to other types of damage, we treated MRC5-SV cells
206 with $KBrO_3$, known to produce a majority of 8-oxo-Guanine lesions [24] and examined the

207 localization of SMN. When treated with $KBrO_3$, SMN shuttling into the nucleolus was also
208 observed (Figure S6A). Additionally, to investigate whether the SMN shuttling is a general event
209 in stress response, we treated the MRC5-SV cells with Cordycepin, an RNAP1 transcription-
210 blocking drug (FigureS6B) and checked the localization of SMN (Figure S6C). After cordycepin
211 treatment (3 hours), SMN shuttling was observed into the nucleolus but with a kinetic that was
212 faster than the one measured after damage induction (Figure S6C).

213 Finally, in order to visualize SMN shuttling in living cells, we produced a Cherry-SMN cell
214 line by transfecting a Cherry-SMN expressing plasmid into the inducible sh6-SMN cell line and
215 selecting a suitable clone that presented the correct SMN localization and level of expression
216 (Figure S7A). After depletion of the endogenous SMN, by induction of the shRNA against SMN
217 with doxycycline, we UV-irradiated and performed time-lapse imaging over the following 48
218 hours, with intervals of 1 hour per image (Figure S7B). During the time-lapse, we could detect
219 the fading of the focal Cherry-SMN signal at around 3 to 6 hours PUVI and the concomitant
220 appearance of Cherry SMN around the nucleoli. This signal lasted at least 24 hours for some cells
221 and disappeared at around 32 hours PUVI with the reappearance of the focal pattern (CBs or
222 Gems) around 40 hours PUVI (Figure S7B).
223

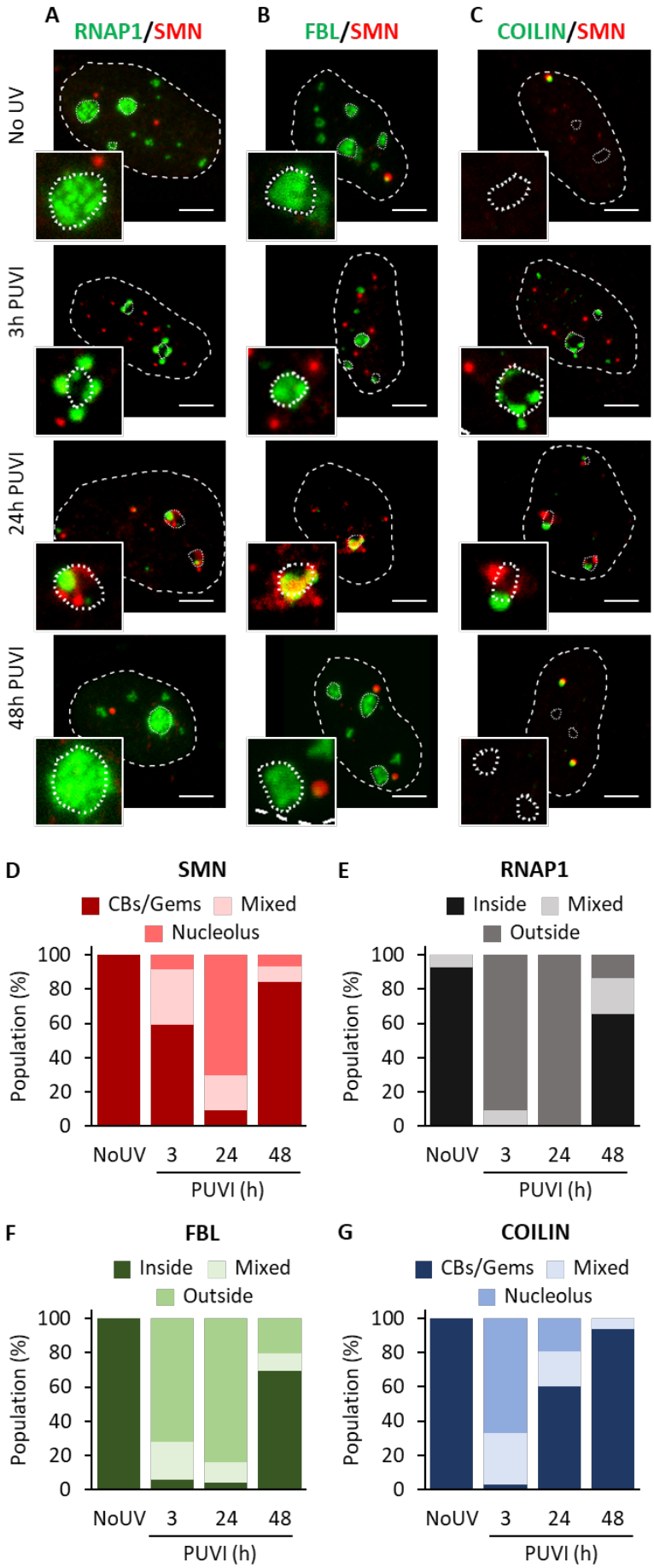
A
RNAP1/SMN
B
FBL/SMN
C
COILIN/SMN
No UV
3h PUVI
24h PUVI
48h PUVI
D
SMN
CBs/Gems
Mixed
Nucleolus
Population (%)
100
80
60
40
20
0
NoUV
3
24
48
PUVI (h)
E
RNAP1
Inside
Mixed
Outside
F
FBL
Inside
Mixed
Outside
G
COILIN
CBs/Gems
Mixed
Nucleolus

225 **Figure 2: Localization of SMN and its partners during DNA repair**

226 *Representative microscopy images of immunofluorescence (IF) assay in MRC5 cells showing,*
227 *after 16J/m² UV-C irradiation, the localization of SMN (red) and* ***(A)*** *RNAP1,* ***(B)*** *FBL or* ***(C)*** *Coilin*
228 *(green) at different times PUVI. Nuclei and nucleoli are indicated by dashed lines and dotted*
229 *lines respectively. Scale bar represents 5 µm.*

230 *Quantification of cells number for localization of* ***(D)*** *SMN and* ***(G)*** *Coilin (in Cajal Bodies [CBs] or*
231 *Gems, at the periphery of the nucleolus or mixed localization), of* ***(E)*** *RNAP1 and* ***(F)*** *FBL (inside*
232 *the nucleolus, outside the nucleolus or mixed localization) at different times PUVI.*

233

234

235 **SMN complex shuttles at the nucleolus after UV irradiation.**

236 Interestingly and differently from Coilin (Figure 2C), at 3h PUVI, SMN is still visible in a
237 focal pattern within the nucleus, reminiscent of Gems. Because of this Coilin-independent
238 localization and to investigate whether SMN shuttles within the nucleolus as an individual protein
239 or as a complex, we investigated whether Gemin2, 3, 4 and 5 (subunits of the SMN complex)
240 change location after UV-irradiation. Remarkably, we could show that Gemin 3, Gemin 4 and
241 Gemin 5 interact with SMN all along this process of displacement and repositioning (Figures 3B,
242 3C, 3D and corresponding quantifications in 3F, 3G and 3H), suggesting that the whole SMN
243 complex is likely involved in the shuttling, or at least some components of the complex. It should
244 be noted that Gemin5 is also present in foci that are SMN negative, these foci were visible all
245 along the nucleolar reorganization process (Figure 3D). Interestingly, Gemin 2 presented a
246 different localization than SMN in both undamaged and damaged conditions. Gemin 2 was found
247 to be present in both CBs/Gems and in the nucleolus in undamaged cells (Figure 3A and
248 corresponding quantification 3E). After damage induction, the proportion of CBs/Gems
249 containing Gemin2 decreased and concomitantly the nucleolar localization increased. To exclude
250 that this nucleolar localization could be the result of a non-specific signal within the nucleolus, we
251 quantified the Gemin2 signal within the nucleolus and observed that the signal increased at 24
252 to 48 hours PUVI (Figure S8). It is important to note that at 48 hours PUVI, most Gemin 2 was still
253 found within the nucleolus (Figure 3E), while SMN was mainly localized in CBs/Gems (Figure 2D).

254 These results might indicate that some SMN partners follow exactly the same localization of SMN
255 during damage-induced nucleolar reorganization, while others might be delayed in some steps
256 of this process.
257

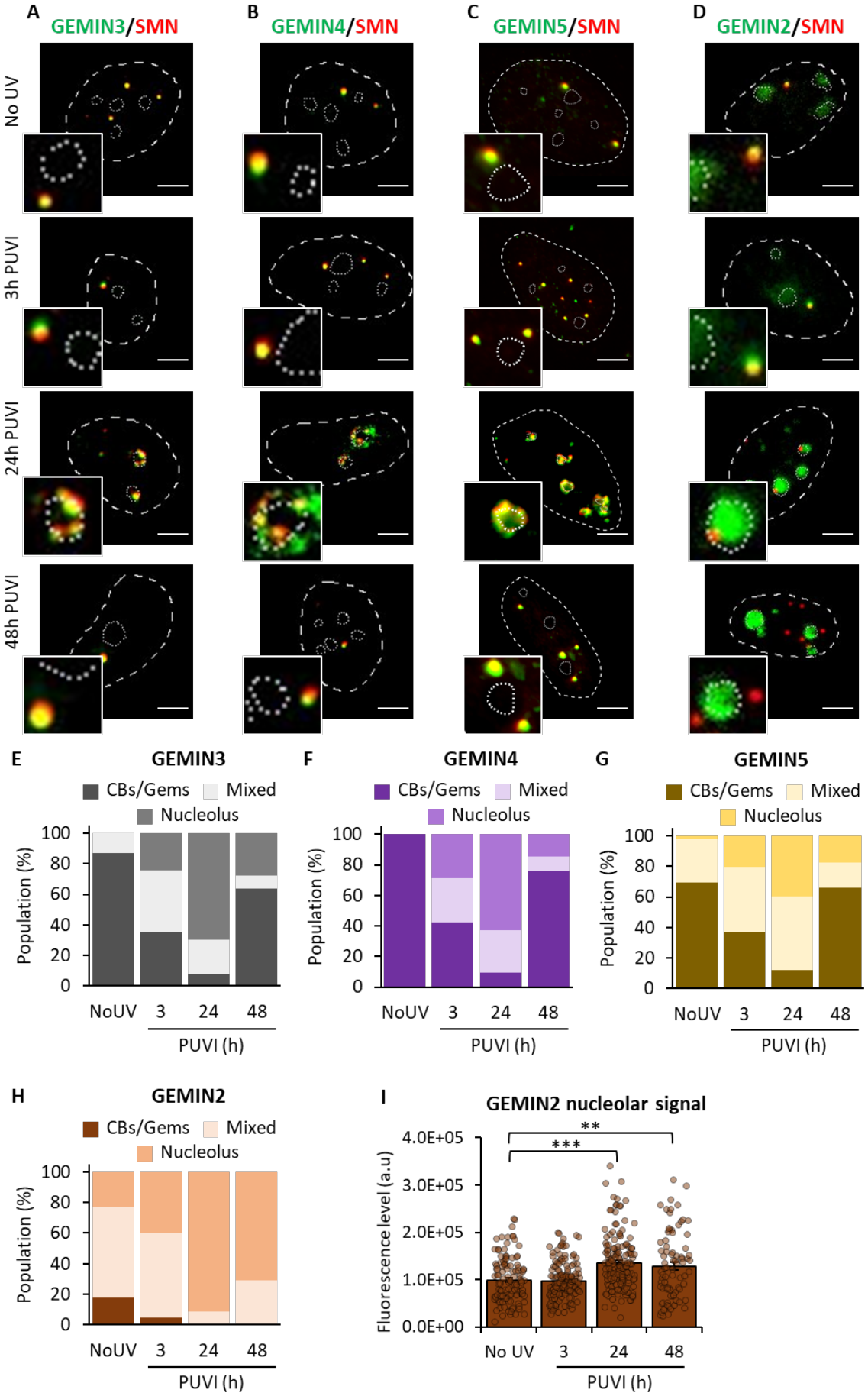
A
GEMIN3/SMN
B
GEMIN4/SMN
C
GEMIN5/SMN
D
GEMIN2/SMN
No UV
3h PUVI
24h PUVI
48h PUVI
E
GEMIN3
F
GEMIN4
G
GEMIN5
CBs/Gems
Mixed
Nucleolus
Population (%)
NoUV
3
24
48
PUVI (h)
H
GEMIN2
I
GEMIN2 nucleolar signal
Fluorescence level (a.u)
4.0E+05
3.0E+05
2.0E+05
1.0E+05
0.0E+00
**
***
No UV

258

259 **Figure 3: Localization of Gemin2, Gemin3, Gemin4 and Gemin5 during DNA repair**

260 *Representative microscopy images of immunofluorescence (IF) assay in MRC5 cells showing,*
261 *after 16J/m² UV-C irradiation, the localization of SMN (red) and* ***(A)*** *GEMIN3,* ***(B)*** *GEMIN3,* ***(C)***
262 *GEMIN4 or* ***(D)*** *GEMIN2 (green) at different times PUVI. Nuclei and nucleoli are indicated by*
263 *dashed lines and dotted lines respectively. Scale bar represents 5 µm.*

264 *Quantification of cells number for localization of* ***(E)*** *GEMIN3,* ***(F)*** *GEMIN4,* ***(G)*** *GEMIN5 or* ***(H)***
265 *GEMIN2 (in Cajal Bodies [CBs] or Gems, at the periphery of the nucleolus or mixed localization),*
266 *at different times PUVI.*

267 ***(I)*** *Quantification of fluorescent signal in the nucleolus from the IF against GEMIN2. Error bars*
268 *represent the standard error of the mean (SEM) obtained from at least 80 cells. P-value of*
269 *Student's test compared to No UV condition. **<0.005, ***<0.001.*

270

271

272 **SMN interacts with FBL, but not with coilin, in the nucleolus after UV irradiation.**

273 We showed that SMN co-localizes with FBL within the nucleolus at 24h PUVI (Figure 2B
274 panel 24h PUVI). To assess the *in vitro* interaction between SMN and FBL after UV-C exposure,
275 we performed a GST pull-down assay using cell extracts untreated or UV-treated at different time
276 points (Figure S8A). We observed that UV treatment seemed to enhance FBL-SMN interactions,
277 while GST alone failed to associate with FBL even if more GST alone than GST-SMN was used in
278 pull-down assays. To confirm this result *in vivo*, we performed a Proximity Ligation Assay (PLA)
279 on wild-type cells at different times PUVI (Figures S8B and S8C). The majority of the cells at 24h
280 PUVI presented a strong PLA signal specifically in the nucleolus between SMN and FBL (Figure
281 S8C) which could be quantified as a specific interaction signal (Figure S8B).

282 Surprisingly, no colocalization was found between SMN and Coilin during the shuttling
283 process, neither at 3 hours nor later on (Figure 2 C). SMN and Coilin did colocalize in CBs before
284 damage induction and 48 hours post damage induction. To confirm this result, we performed
285 PLA on wild-type cells at different times PUVI (Figures S8D and S8E) and we could not detect any
286 added interaction/proximity between SMN and Coilin during damage-induced nucleolar
287 reorganization.

288

289

290 **Coilin is required for SMN import into the nucleolus and for the nucleolar rearrangement**
291 **following UV-C exposure.**

292 We observed that Coilin localized to the nucleolus during UV damage (at 3h PUVI) prior
293 to SMN (Figures 2C and 2G). These results led us to hypothesize that Coilin might be the factor
294 that recruits SMN to the nucleolus. To test this idea, we depleted cells of Coilin by using a pool
295 of four specific siRNAs and two individual siRNAs (Figure S9A) and performed IF of SMN and
296 RNAP1 on wild-type cells before damage and at different time PUVI (Figure 4A) in the presence
297 or absence of Coilin. Interestingly, what could be noticed was that the number of cells presenting
298 SMN foci was drastically diminished when Coilin was downregulated (Figure S9B), this result is
299 consistent with the fact that CBs are dismantled in the absence of Coilin. This would mean that,
300 in this condition, visible SMN foci would more likely correspond to Gems. To investigate whether
301 Gems would shuttle to the nucleolus, we excluded from the quantification cells that did not
302 present SMN foci. Our results show that, without Coilin, the shuttling of SMN within the nucleolus
303 is impaired and SMN remains mostly in Gems (Figure 4A and corresponding quantification
304 Figures 4C and S9C). Consequently, in cells deficient for Coilin, the nucleolar reorganization after
305 DNA damage and repair is not restored and RNAP1 remains at the periphery of the nucleolus at
306 48h PUVI (Figures 4A and 4C and S9C), indicating that the shuttling of SMN and the presence of
307 Coilin are both important to ensure the re-establishment of the nucleolar reorganization.

308 To investigate whether the absence of Coilin would impact the interaction between SMN
309 and FBL, we performed PLA and IF of SMN and FBL on wild-type cells before damage and at
310 different times PUVI in the presence or absence of Coilin (Figures 4D, 4E and 4F). Our results
311 show that without Coilin, SMN remains outside of the nucleolus and no co-localization with FBL
312 was observed (Figure 4D). As a consequence, the interaction between SMN and FBL observed
313 at 24h PUVI (Figures S8B and S8C) is lost in Coilin-depleted cells (Figures 4E and 4F).

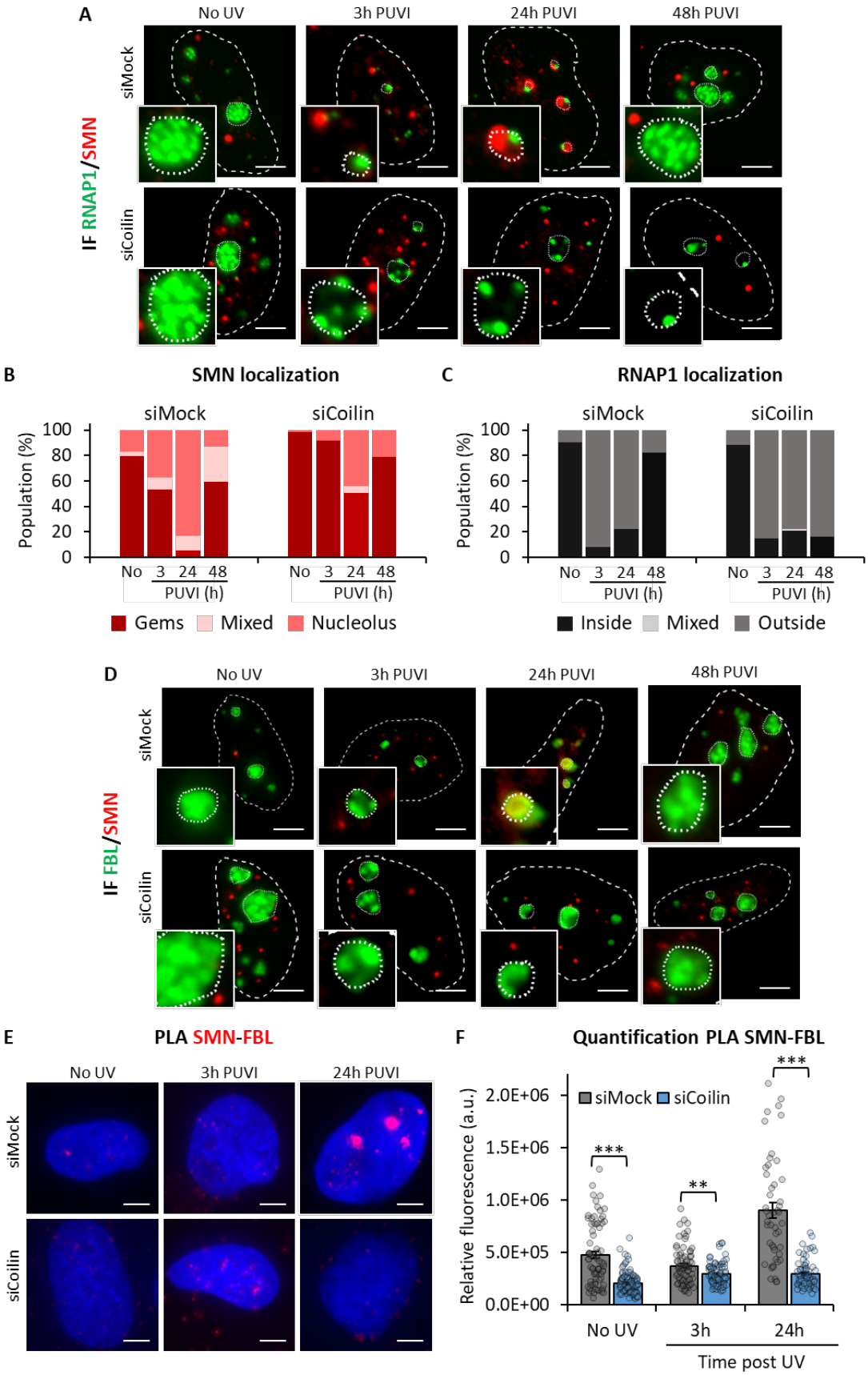
A
No UV
3h PUVI
24h PUVI
48h PUVI
siMock
siCoilin
IF RNAP1/SMN
B
SMN localization
siMock
siCoilin
Population (%)
100
80
60
40
20
0
No
3
24
48
PUVI (h)
Gems
Mixed
Nucleolus
C
RNAP1 localization
Inside
Mixed
Outside
D
IF FBL/SMN
E
PLA SMN-FBL
F
Quantification PLA SMN-FBL
Relative fluorescence (a.u.)
2.0E+06
1.5E+06
1.0E+06
5.0E+05
0.0E+00
***
**
No UV
3h
24h
Time post UV

314

315 **Figure 4: SMN shuttling is Coilin-dependent**

316 ***(A and D)*** *Representative microscopy images of immunofluorescence (IF) assay showing the*
317 *localization of SMN (red) and* ***(A)*** *RNAP1 or* ***(D)*** *FBL (green) at different times PUVI in cells*
318 *transfected with siMock or siCoilin pool. Nuclei and nucleoli are indicated by dashed lines and*
319 *dotted lines respectively. Scale bar: 5µm.* ***(B and C)*** *Quantification of cells number for localization*
320 *of* ***(B)*** *SMN (in Cajal Bodies [CBs] or Gems, at the periphery of the nucleolus or mixed localization)*
321 *and* ***(C)*** *RNAP1 (inside the nucleolus, outside the nucleolus or mixed localization) at different*
322 *times PUVI in cells transfected with siMock or siCoilin pool.* ***(E)*** *Representative microscopy*
323 *images of PLA showing the interaction between SMN and FBL at different times PUVI in cells*
324 *transfected with siMock or siCoilin. Scale bar: 5µm.* ***(F)*** *Quantification of fluorescent signal in the*
325 *nucleus against the couple SMN-FBL from PLA experiment in cells transfected with siMock or*
326 *siCoilin pool after UV-C irradiation. P-value of Student's test compared to siMock condition.*
327 ***<0.005, ***<0.001.*

328

329

330 **FBL is required for SMN export from the nucleolus and for the nucleolar rearrangement**
331 **following UV-C exposure.**

332 As Coilin, FBL is an essential partner of SMN and a nucleolar protein that can methylate
333 rDNAs and Histones within the nucleolus [21,25]. We showed that FBL and SMN interact in cell
334 extracts by GST (Figures S5E and S8A) and *in vivo* by PLA (Figures S8B and S8C), notably stronger
335 after SMN shuttling into the nucleolus (24h PUVI). As the SMN shuttling is dependent on Coilin
336 (Figure 4), we wondered whether FBL depletion would also play a role in this shuttling process.
337 To test this hypothesis, we depleted cells of FBL by using a specific siRNA pool (Figure S10A) or
338 2 independent siRNAs (Figure S10B) and performed IF of SMN and RNAP1 on wild-type cells
339 before damage and at different times PUVI (Figure 5A, corresponding quantifications in Figures
340 5B and 5C) in presence or absence of FBL. Our results show that without FBL, the shuttling of
341 SMN within the nucleolus is altered, namely SMN localizes at the periphery of the nucleolus
342 already at 3h PUVI and stays at the periphery of the nucleolus at all time points (Figures 5A, 5B
343 and S10B). Importantly, in cells deficient for FBL, the nucleolar reorganization after DNA damage

344 and repair is not restored and RNAP1 remains at the periphery of the nucleolus at 48h PUVI
345 (Figures 5A, 5C and S10C), indicating that the shuttling of SMN within the nucleolus and the
346 presence of FBL are both important to ensure the re-establishment of the nucleolar
347 reorganization.

348 To verify if and how the absence of FBL affects the localization and interaction between
349 SMN and Coilin, we performed IF and PLA of SMN and Coilin on wild-type cells before damage
350 and at different times PUVI (Figures 5D, 5E and 5F) in the presence or absence of FBL. Our results
351 show that, without FBL, the interaction between SMN and Coilin is detectable at all times PUVI
352 (Figures 5E and 5F) and both SMN and Coilin are localized at the periphery of the nucleolus
353 already at 3h PUVI, this localization does not change at 24h or 40h PUVI (Figure 5D). These
354 findings show that FBL is also a critical player in SMN shuttling and in nucleolar reorganization
355 following UV irradiation and DNA repair.

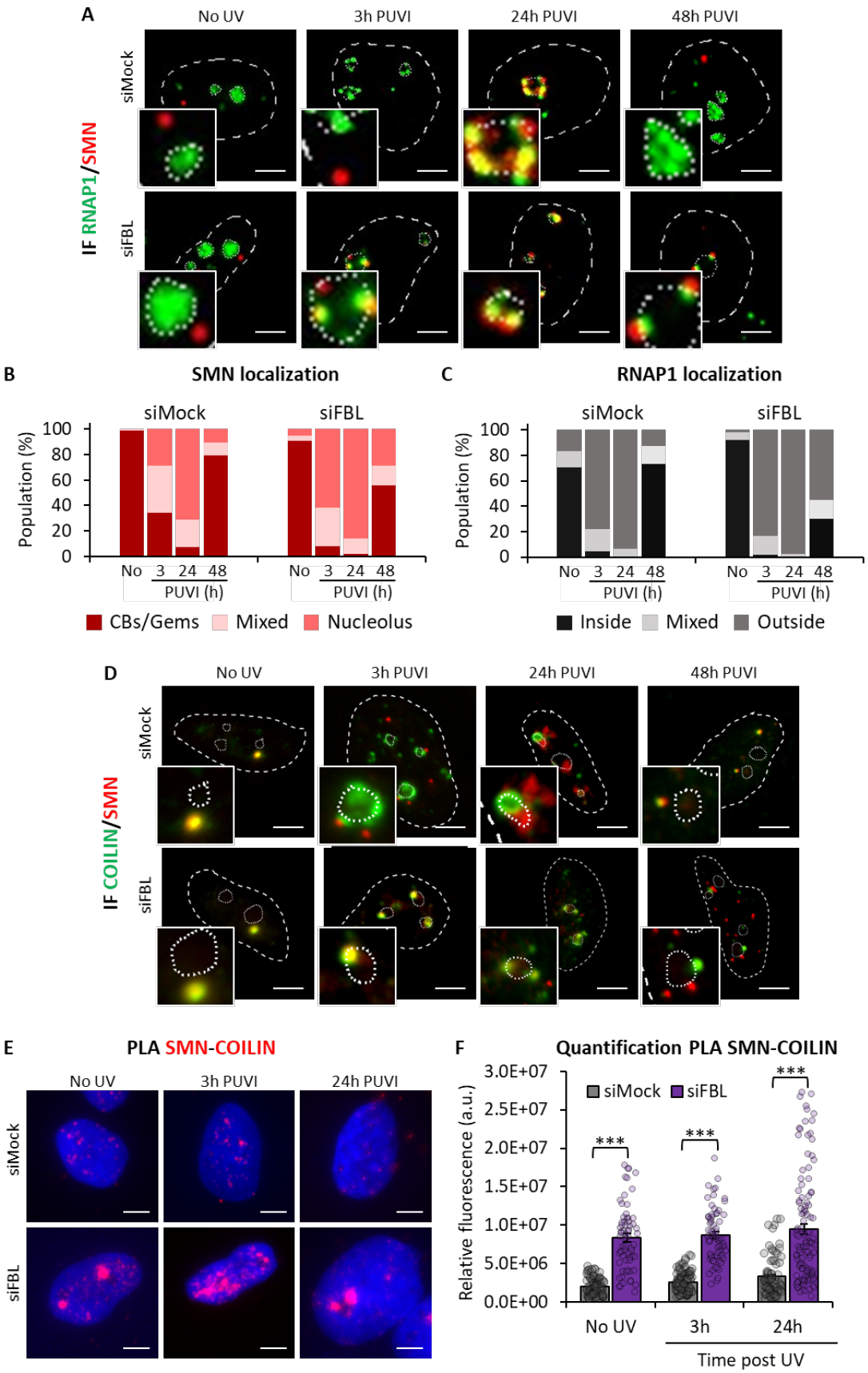
A
No UV
3h PUVI
24h PUVI
48h PUVI
siMock
siFBL
IF RNAP1/SMN
B
SMN localization
siMock
siFBL
Population (%)
100
80
60
40
20
0
No
3
24
48
PUVI (h)
CBs/Gems
Mixed
Nucleolus
C
RNAP1 localization
Inside
Mixed
Outside
D
IF COILIN/SMN
E
PLA SMN-COILIN
F
Quantification PLA SMN-COILIN
Relative fluorescence (a.u.)
3.0E+07
2.5E+07
2.0E+07
1.5E+07
1.0E+07
5.0E+06
0.0E+00
***
No UV
3h
24h
Time post UV

356

357 **Figure 5: The release of SMN from the nucleolus is FBL-dependent**

358 ***(A and D)*** *Representative microscopy images of immunofluorescence (IF) assay showing the*
359 *localization of SMN (red) and* ***(A)*** *RNAP1 or* ***(D)*** *COILIN (green) at different times PUVI in cells*
360 *transfected with siMock or siFBL pool. Nuclei and nucleoli are indicated by dashed lines and*
361 *dotted lines respectively. Scale bar: 5µm.* ***(B and C)*** *Quantification of cells number for localization*
362 *of* ***(B)*** *SMN (in Cajal Bodies [CBs] or Gems, at the periphery of the nucleolus or mixed localization)*
363 *and* ***(C)*** *RNAP1 (inside the nucleolus, outside the nucleolus or mixed localization) at different*
364 *times PUVI in cells transfected with siMock or siFBL pool.* ***(E)*** *Representative microscopy images*
365 *of PLA showing the interaction between SMN and COILIN at different times PUVI in cells*
366 *transfected with siMock or siFBL pool. Scale bar: 5µm.* ***(F)*** *Quantification of fluorescent signal in*
367 *the nucleus against the couple SMN-COILIN from PLA experiment in cells transfected with*
368 *siMock or siFBL pool after UV-C irradiation. P-value of Student's test compared to siMock*
369 *condition. ***<0.001.*

370

371

372 **SMN mutants are deficient in nucleolar reorganization after DNA damage induction and repair**

373 SMN protein has different domains that are important for its functionality, interactions
374 with partners and stability (Figure S5F). In order to study how different SMN domains impact the
375 nucleolar reorganization function of SMN, we have focused on two SMN mutants: (i) a mutant in
376 the Tudor domain (E134K) and (ii) a mutant in the YG domain (Y272C). The Tudor domain is
377 important for the interaction of SMN with FBL and Coilin [21], while the YG domain is essential for
378 the oligomerization of SMN [26] which is more stable than the monomeric form.

379 We investigated whether these mutated SMN might have a defect in nucleolar
380 reorganization after DNA damage induction or in the shuttling of SMN to and/or from the
381 nucleolus. We produced three GFP-SMN cell lines by transfecting into the inducible sh6-SMN
382 cell line (i) a wild-type GFP-tagged SMN (hereafter GFP-SMN); (ii) a mutant GFP-tagged SMN,
383 bearing the mutation in the Tudor domain E134K (hereafter GFP-SMN^{E134K}); (iii) a mutant GFP-
384 tagged SMN, bearing the mutation in the YG domain Y272C (hereafter GFP-SMN^{Y272C}). After the
385 selection of suitable clones, we verified the amount of GFP-SMN and the mutant SMN proteins

386 produced and we could determine that the amount of mutant SMN was lower than the GFP-SMN
387 protein (Figure S11A). After depletion of the endogenous SMN, by induction of the sh6-SMN
388 RNA, we UV-irradiated SMN wild type and mutant expressing clones and we performed IF against
389 RNAP1 coupled to the direct visualization of the GFP-SMN, GFP-SMN^{E134K} or GFP-SMN^{Y272C}
390 signal. Wild-type and mutant SMN proteins could be visualized in CBs/Gems in undamaged cells
391 (Figures S11B and S11C). Nevertheless, the Tudor mutant GFP-SMN^{E134K} expressing cells failed
392 to restore CBs/Gems at 48h PUVI and the nucleolar reorganization was not restored, RNAP1
393 remaining at the periphery of the nucleolus at 48h PUVI (Figures S11B, S11C and S11D).
394 Interestingly, these results are reminiscent of the results observed in the absence of FBL (Figures
395 5A, 5B and 5C). The YG mutant GFP-SMN^{Y272C} failed to properly shuttle to the nucleolus and
396 remained mostly in CBs/Gems all along the nucleolar reorganization process (Figures S11B and
397 S11C) and the nucleolar reorganization was not restored at 48h PUVI (Figures S11B and S11D).
398 These results are reminiscent of the results observed in the absence of COILIN (Figures 4A, 4B
399 and 4C). To resume, both SMN mutants studied, show that a functional SMN is needed to
400 properly ensure nucleolar homeostasis after DNA damage induction and that in different ways
401 SMN shuttling is perturbed by these mutations.
402
403
404 **PRMT1 activity mediates the nucleolar shuttling of SMN**
405 One of the activities of SMN is to bind, via the Tudor domain, Arginine methylated
406 proteins [27,28]. Arginine methylation is a widespread post-translational modification that can occur
407 in histones and non-histone proteins [29–32]. The enzymes catalyzing the transfer of a methyl group
408 to Arginine residues are part of a family called the PRMTs (Protein Arginine Methyl Transferases).
409 PRMTs can mono-methylate Arginine residues (MMA) or di-methylate Arginine residues either
410 symmetrically (SDMA) or asymmetrically (ADMA). Because these proteins affect SMN functions
411 but also the interaction of SMN with Coilin [33], we wondered whether one of the PRMTs could
412 affect, disturb or enhance SMN shuttling after DNA damage. Using GST pull-down assay, we
413 observed that PRMT1 interacts with SMN (Figure S12A). We thus decided to deplete cells from
414 PRMT1 by siRNA silencing (Figure S12B) and performed IF against SMN and FBL. We found that

415 PRMT1 inhibited the shuttling of SMN to the nucleolus (Figures 6A and 6B). In fact, in PRMT1-
416 depleted cells, SMN remains mostly in CBs/Gems. This SMN localization after DNA damage is
417 reminiscent of the one observed in Coilin-depleted cells (Figure 4A).

418 To verify whether the perturbation of SMN shuttling observed in Figure 6A is due to the
419 physical depletion of PRMT1 or the inhibition of the ADMA methylase activity, we treated the
420 cells with the PRMT-class I specific inhibitor MS023 [34] and the more specific and potent PRMT1
421 inhibitor, Furamidine[35] (Figures 6D, 6E, S12C and S12D) prior to DNA damage and IF assays. We
422 could verify that the inhibition of the methylase activity of PRMTs from class I and specifically of
423 PRMT1 perturbs SMN shuttling (Figures 6D, 6E and S12C) and that SMN remains mostly in
424 CBs/Gems as when PRMT1 is depleted (Figure 6A). Because the SMN complex requires the
425 protein arginine methyltransferase 5 (PRMT5) to assemble Sm core structures of spliceosomal U-
426 rich small nuclear ribonucleoprotein particles[36], we investigated whether depletion of PRMT5
427 would affect SMN shuttling to the nucleolus. We down-regulated PRMT5 by siRNA (Figure S13D),
428 induced DNA damage and perform IF against SMN and RNAP1 at different times PUVI (Figure
429 S13A). Our results show that depletion of PRMT5 does not influence SMN shuttling (Figures S13A
430 and S13B), nor the nucleolar homeostasis after DNA damage and repair (Figures S13A and S13C).

431 To investigate how the depletion of PRMT1 affects the interactions between SMN and its
432 partners (Coilin and FBL), we performed PLA assays and measured a stronger interaction of SMN
433 and FBL before damage induction and at 3h PUVI which corresponds with the beginning of SMN
434 shuttling at the nucleolus (Figures 7A and 7B). We also quantified a stronger interaction of SMN
435 with Coilin when PRMT1 is depleted (Figures 7C and 7D) before damage induction and up to
436 48h PUVI.

437 Remarkably, we showed by IF that PRMT1 is also shuttling during nucleolar reorganization
438 in wild-type cells and could be detected at 6h and up to 48h PUVI within the nucleolus or at the
439 periphery of the nucleolus (Figures S14A and S14B). Importantly, the shuttling of PRMT1 at the
440 nucleolus is dependent on the SMN protein as in SMN-depleted cells (Sh6-SMN), PRMT1 is not
441 detected inside the nucleoli but remains mainly nuclear or localized at the periphery of the
442 nucleolus (Figures S14A and S14B).

443 Interestingly, we could quantify an increased level of PRMT1 after damage induction and
444 we could show that this increase is partially dependent on the presence of a functional SMN
445 (Figures S14C, S15A and S15B).

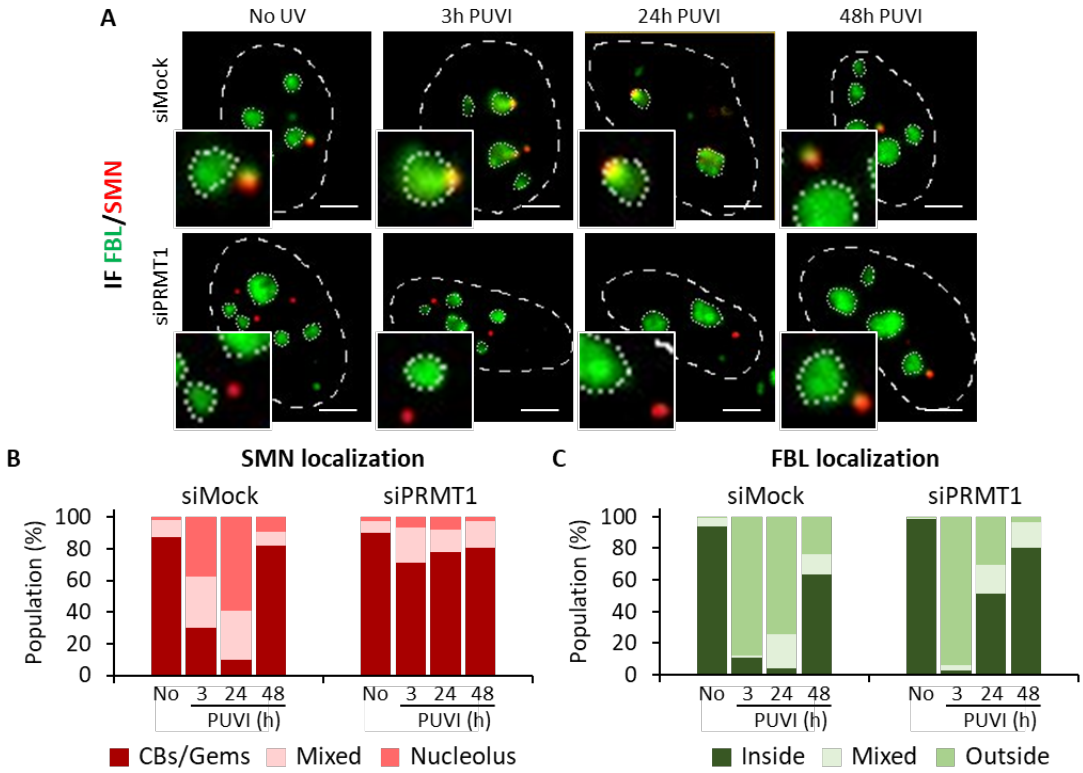
A
No UV
3h PUVI
24h PUVI
48h PUVI
siMock
siPRMT1
IF FBL/SMN
B
SMN localization
siMock
siPRMT1
Population (%)
100
80
60
40
20
0
No
3
24
48
PUVI (h)
CBs/Gems
Mixed
Nucleolus
C
FBL localization
siMock
siPRMT1
Population (%)
Inside
Mixed
Outside

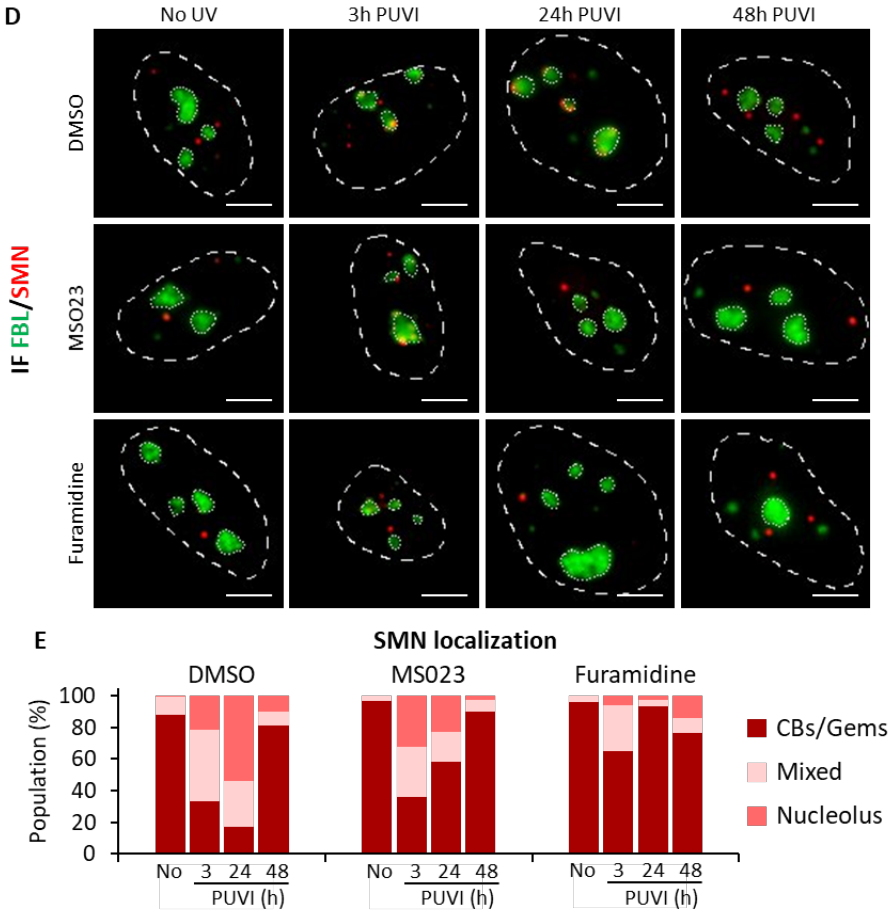
D
No UV
3h PUVI
24h PUVI
48h PUVI
DMSO
MSO23
Furamidine
IF FBL/SMN
E
SMN localization
DMSO
MS023
Furamidine
Population (%)
100
80
60
40
20
0
No
3
24
48
PUVI (h)
CBs/Gems
Mixed
Nucleolus

446

447 **Figure 6: PRMT1 activity mediates the nucleolar shuttling of SMN**

448 ***(A)*** *Representative microscopy images of immunofluorescence (IF) assay showing the localization*
449 *of SMN (red) and FBL (green) at different times PUVI in cells transfected with siMock or siPRMT1*
450 *pool. Nuclei and nucleoli are indicated by dashed lines and dotted lines respectively. Scale bar:*
451 *5µm.* ***(B and C)*** *Quantification of cells number for localization of* ***(B)*** *SMN (in Cajal Bodies [CBs]*
452 *or Gems, at the periphery of the nucleolus or mixed localization) and* ***(C)*** *FBL (inside the*
453 *nucleolus, outside the nucleolus or mixed localization) at different times PUVI in cells transfected*
454 *with siMock or siPRMT1 pool.* ***(D)*** *Representative microscopy images of IF assay showing the*
455 *localization of SMN (red) and FBL (green) in MRC5 cells treated with DMSO, MS023 or*
456 *Furamidine followed by 16J/m² UV-C irradiation. Nuclei and nucleoli are indicated by dashed*
457 *lines and dotted lines respectively. Scale bar: 5µm.* ***(E)*** *Quantification of cells number for*
458 *localization of SMN (in Cajal Bodies [CBs] or Gems, at the periphery of the nucleolus or mixed*
459 *localization) at different times PUVI in cells treated with DMSO, MS023 or Furamidine.*

460

461

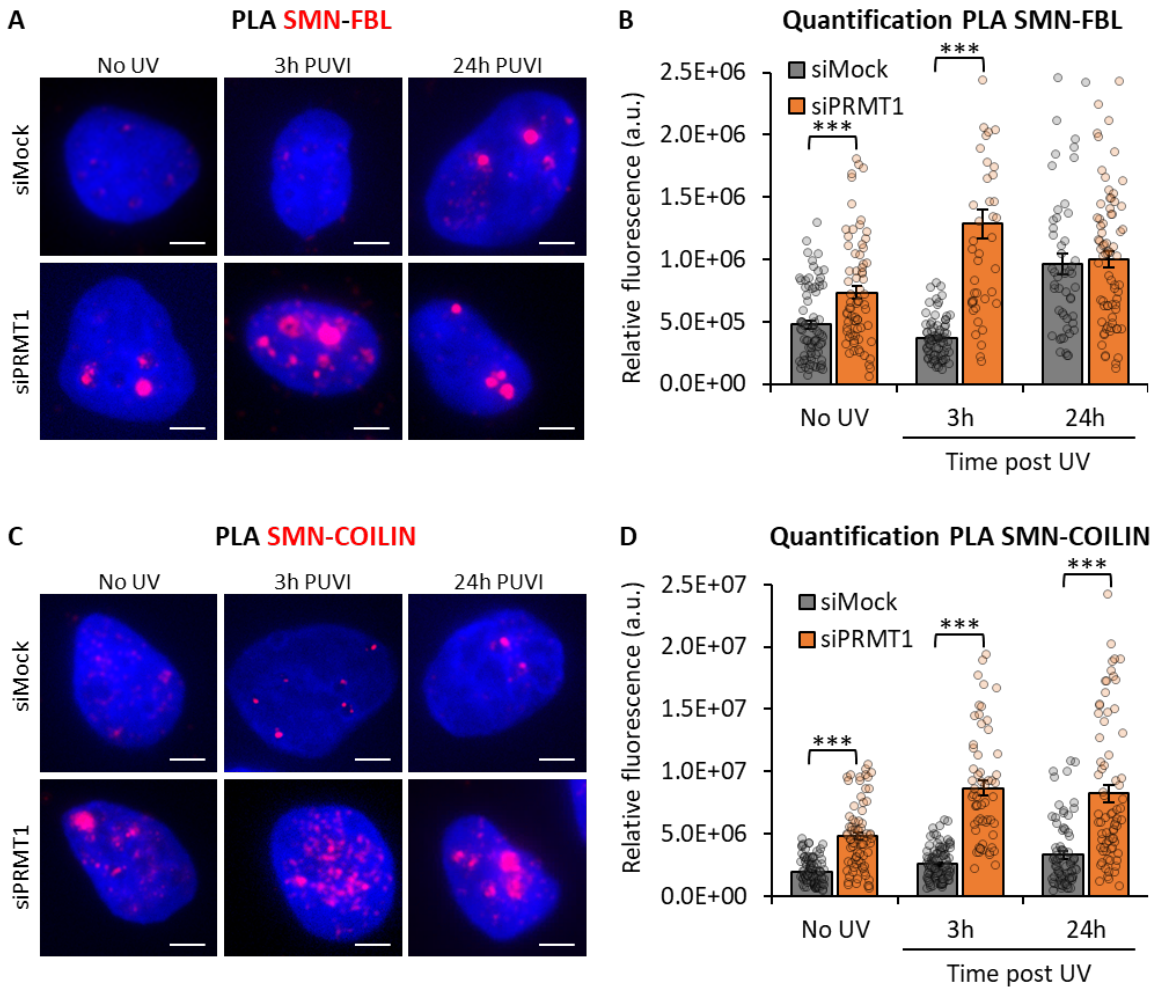

Figure 7: PRMT1 remodels the interaction of SMN with FBL and COILIN

(A and C) *Representative microscopy images of PLA showing the interaction between SMN and FBL* ***(A)*** *or between SMN and COILIN* ***(C)*** *at different times PUVI in cells transfected with siMock or siPRMT1 pool. Scale bar: 5µm.* ***(B and D)*** *Quantification of fluorescent signal in the nucleus against the couple SMN-FBL* ***(B)*** *or SMN-COILIN* ***(D)*** *from PLA experiment in cells transfected with siMock or siPRMT1 pool after UV-C irradiation. P-value of Student's test compared to siMock condition. ***<0.001.*

SMN cells are sensitive to DNA damage

473 We demonstrated that a functional SMN is important for proper nucleolar homeostasis
474 after DNA damage repair and wondered whether this newly discovered function could have a
475 biological consequence on SMN cells and *in fine* on SMA patients. In order to investigate whether
476 DNA damage could impact the survival of SMN cells we performed clonogenic assays on sh6-
477 SMN cells with and without induction of the sh expression and compared the results with a DNA
478 repair-deficient cell lines (CS1AN-SV) mutated in the CSB protein, involved in transcription
479 coupled-NER (Figure 8A). Our results show that SMN-depleted cells are moderately sensitive to
480 UV damage as their sensitivity to UV irradiation is intermediate between an SMN wild-type cell
481 line and a DNA repair-deficient cell line.
482 Because we demonstrated that SMN shuttling is also happening during oxidative damage
483 repair (Figure S6A), we wondered whether SMN cells would be sensitive to chronic oxidative
484 damage. We usually culture rodents, human patients or mutated cell lines in physioxia conditions
485 (3% of oxygen) to avoid the supraphysiological oxygen levels disturbing normal cellular
486 metabolism and increasing the cellular concentration of reactive oxygen species [37]. To induce
487 chronic oxidative damage in SMN-depleted cells, we culture them in a standard incubator at 20%
488 oxygen and compare their ability to form colonies. As with many established cell lines, Human
489 SV40-immortalized fibroblasts MRC5 (MRC5-SV) have a better clonogenicity in physioxia
490 conditions (Figure 8B). However, MRC5-SV expressing shRNA SMN has a decreased
491 clonogenicity compared to MRC5-SV that expresses a mock shRNA (Figure 8B), which
492 demonstrates that the absence of SMN *per se* hinders the ability of cells to form clones.
493 Importantly, when SMN-depleted cells are grown in supraphysiological oxygen levels their
494 clonogenicity is more drastically reduced, compared with the physioxia culture conditions (Figure
495 8C).
496

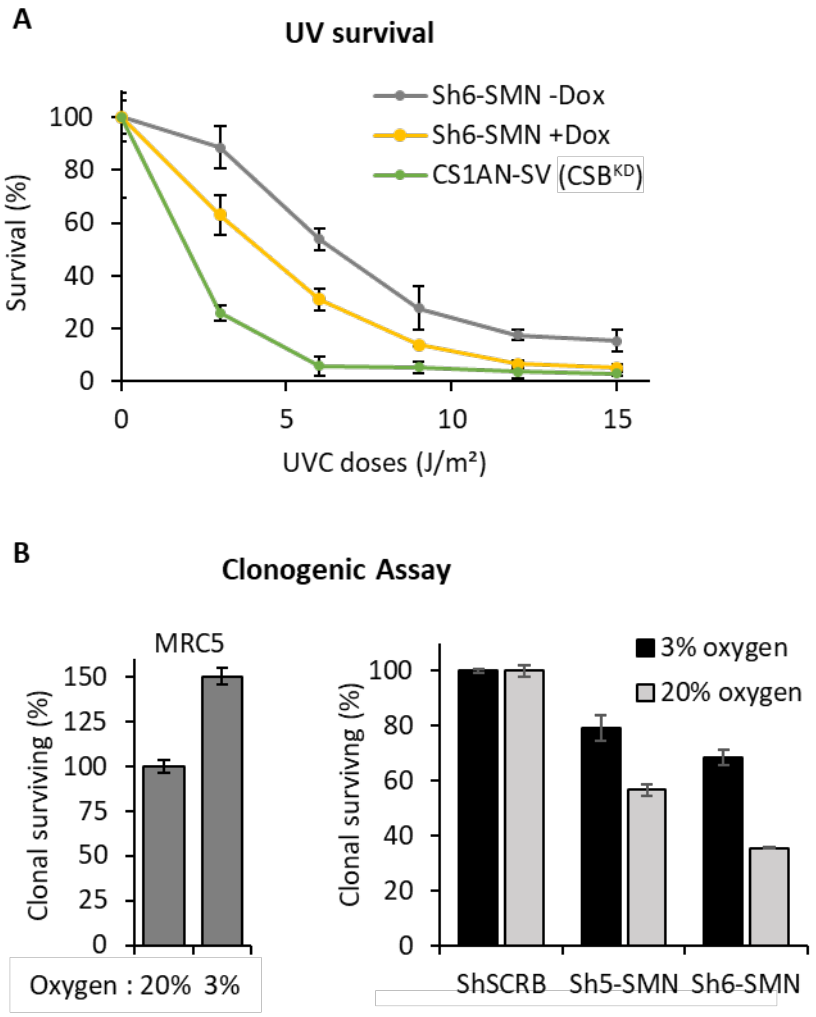

497

498 **Figure 8: SMN-deficient cells are sensitive to DNA damage**

499 ***(A)*** *Survival curve as determined by the colony-forming ability to UV-C of cells expressing (+Dox) or not (-*

500 *Dox) Sh6-SMN.* ***(B)*** *Clonogenic assay of cells cultured with different quantities of oxygen (3% or 20%) in*

501 *the presence (MRC5 or ShSCRB) or absence of SMN (Sh5-SMN and Sh6-SMN).*

502

503

504

505 ## DISCUSSION

506 One of the most fascinating and nearly unexplored areas in the DNA repair field is how
507 cells restore their cellular activities after the completion of all the reactions that allow cells to
508 eliminate DNA lesions. Most DNA lesions block transcription and replication [5] and although we
509 have extensive knowledge of how cells recognize and repair DNA lesions, very little is known
510 about how cells restart these cellular processes. In post-mitotic cells, restoration of the damage-
511 induced block of transcription is essential for cell survival.

512 We have previously shown that RNAP1 transcription is blocked after UV lesions and that
513 TC-NER pathway is responsible for the repair of UV-lesions on ribosomal DNA [8]. Importantly, UV-
514 damages impact the organization of the nucleolus and during DNA repair both nucleolar DNA
515 and RNAP1 are displaced at the periphery of the nucleolus [8]. Interestingly, although RNAP1
516 transcription restarts when UV-lesions on the transcribed strand are repaired, the return of the
517 RNAP1 within the nucleolus is dependent on the proper repair of DNA lesions on the
518 untranscribed nucleolar DNA [8]. In this particular case (GG-NER deficient cells), RNAP1
519 transcription restarts in a non-canonical compartment, the periphery of the nucleolus, and this
520 anomaly might influence the proper ribosome biogenesis. Therefore, restoring the proper
521 nucleolar structure and organization might be important for cellular viability or the efficiency of
522 cellular processes. The recovery of a normal nucleolar structure after DNA damage repair is not
523 a passive process and requires the presence of some key proteins [9], although their exact
524 mechanistic role has not been established yet.

525 In a quest to find the exact molecular mechanism for the re-establishment of the nucleolar
526 organization after DNA repair completion, we set up a best-candidate approach that guided us
527 to inspect the consequences of different nucleolar proteins' interactors depletion. One of these
528 candidates was the protein SMN, which is a particularly interesting protein to scrutinize because
529 of the known interaction with the nucleolar protein FBL via its Tudor domain [17].

530 SMN is part of a multiprotein complex that includes Gemins2-8 and Unrip [38] and acts like
531 a molecular chaperone needed to assemble small ribonucleoproteins (snRNPs) which are part of
532 the spliceosome [39] and small nucleolar ribonucleoprotein particles (snoRNPs) involved in

533 posttranscriptional processing of ribosomal RNA [21]. Additionally, SMN has been also found
534 implicated in transcription [40], histone mRNA processing [41], mRNAs trafficking [42] and translation [43].
535 We have shown here that SMN plays a role in nucleolar homeostasis after DNA repair
536 completion. In fact, silencing or mutations (Tudor domain and oligomerization mutants) of the
537 SMN protein hinder the proper return of RNAP1 within the nucleolus (Figure 9), despite the
538 restart of RNAP1 transcription (Figure 1, Figures S2, S3 and S11). Contrary to what has been
539 observed in GG-NER deficient cells, the RNAP1 mislocalization after DNA repair completion is
540 not induced by the presence of unrepaired DNA lesions because we could show that SMN
541 deficient cells are proficient in the NER pathway, repairing UV-lesions on both transcribed and
542 untranscribed regions of the genome (Figure S4).
543 The multifunctional SMN is localized in both the cytoplasm and in nuclear bodies (Cajal
544 Bodies and Gems) and in addition, SMN can also be detected in the nucleolus of neurons [16]
545 although the function of SMN in nucleolus remains enigmatic. Interestingly, during the process
546 of nucleolar reorganization, we observed a shuttling of SMN from CBs/Gems to the periphery of
547 the nucleolus or within the nucleolus during RNAP1 displacement and a return to CBs/Gems after
548 the RNAP1 repositioning (Figures 2, 9). SMN shuttles to the nucleolus together with its partners
549 Gemin 2, Gemin 3, Gemin 4 and Gemin 5 (Figure 3). While Gemin 3 and 4 followed the same
550 SMN localization, the classical SMN partner Gemin 2 [44] was observed to have both CBs/Gems
551 and nucleolar localization. While SMN/Gemin2 foci disappeared during RNAP1 displacement,
552 the nucleolar signal of Gemin 2 increased reaching the maximum after RNAP1 repositioning and
553 Gemin2 foci did not reappear. This result might suggest that SMN complex is not exactly the
554 same in CBs/Gems when performing snRNPs assembly and in the nucleolus during DNA repair-
555 induced nucleolar reorganization. These results also suggest that the restoration of fully
556 functional CBs/Gems containing Gemin2 might be delayed in time, probably further delaying the
557 restoration of the other functions of the SMN complex. Notably, Gemin 5 was observed in both
558 SMN positive and negative foci which could be because a large fraction of Gemin5 protein is
559 found outside of the SMN complex [45]. Interestingly, SMN negative foci of Gemin5 were present
560 at any time point throughout the nucleolar reorganization process, which might indicate that SMN

561 negative foci of Gemin5 do not participate in the shuttling of SMN complex and in nucleolar
562 homeostasis.

563 SMN shuttling happens in replicative and post-mitotic cells (motoneurons) and in different
564 stress situations: UV-induced DNA damage, RNAP1 transcriptional block and drug-induced
565 oxidative damage. Notably, we should highlight that the kinetics of SMN shuttling might vary
566 depending on different types of stresses but also on the culture conditions, the amount and
567 quality of serum, supraphysiological oxygen levels and the type of culture media. The kinetic of
568 SMN shuttling should be defined for each type of stress/damage and culture condition.

569 SMN shuttling is dependent on both Coilin and FBL (Figures 4, 5 and 9). In Coilin-
570 depleted undamaged cells, we observed a high number of cells in which no CBs or other foci
571 were visible, this might be because, without Coilin, CBs are disrupted and just Gems are visible.
572 In the absence of Coilin, we observe an increased number of Gems and the number of cells in
573 which SMN is at the nucleolus is reduced. Interestingly, in Coilin-depleted cells RNAP1
574 repositioning is hindered, indicating that in the absence of Coilin nucleolar reorganization is
575 compromised. In FBL-depleted cells, SMN remains at the periphery of the nucleolus at all time
576 points and RNAP1 does not recover the proper localization within the nucleolus but remains at
577 the periphery of the nucleolus.

578 Because FBL interacts with SMN via its Tudor domain [17] and SMN interacts mainly with
579 methylated arginine residues, we explored the possibility that one of the PRMTs would be
580 responsible for SMN shuttling within the nucleolus. Indeed, the activity of PRMT1, responsible
581 for ADMA, is essential to recruit SMN to the nucleolus (Figures 6 and 9). In contrast, depletion of
582 PRMT5, which is responsible for the assembly of Sm proteins to the SMN complex did not
583 influence the shuttling of SMN, probably indicating that the SMN function in nucleolar
584 homeostasis is independent of the snRNPs biogenesis process[46] (Figure S13).

585 Interestingly, depletion of Coilin, FBL and PRMT1 also modifies the interactions between
586 SMN, Coilin and FBL, by increasing their proximities (Figures 5, 6 and 7) which might indicate
587 that specific methylations are important to maintain an equilibrium of interactions between these
588 three partners.

589 Remarkably PRMT1 shuttles within the nucleolus after DNA damage induction as SMN
590 (Figure 7). This shuttling within the nucleolus is SMN-dependent. Although we do not know if the
591 substrate of PRMT1 is a protein that directly interacts with SMN, we showed that methylation is
592 essential for SMN shuttling. It is plausible to assume that because FBL is methylated by PRMT1
593 [47], FBL might be the substrate methylated during the process of RNAP1 repositioning within the
594 nucleolus after the completion of DNA repair.
595

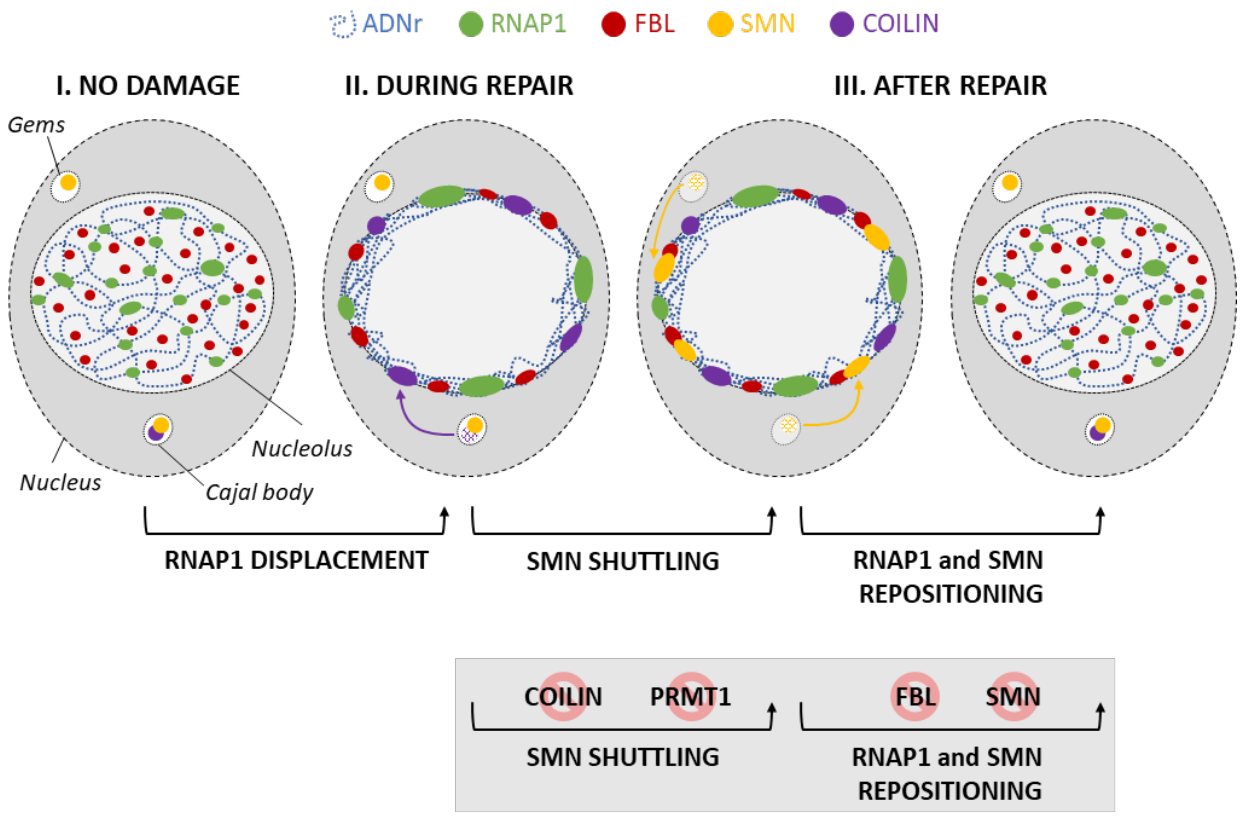

596
597 **Figure 9: SMN shuttling during DNA damage/repair dependent nucleolar reorganization.**
598
599 In the future years, it will be important to unveil the precise mechanism of action of SMN
600 within the nucleolus, by investigating what are the partners of SMN in this organelle after DNA
601 damage and how they function together with SMN, how CBs/Gems disassemble and reassemble,
602 how they restore their activity and what are the consequences on splicing, ribosome biogenesis
603 and finally translation fidelity. More generally, it will be important to continue to study how cells
604 maintain and/or restore nucleolar homeostasis after cellular stresses, such as DNA damage.

605 We believe that our study will also open new avenues of research that could improve the
606 well-being of SMA patients. As for other multifunctional proteins, it is difficult to identify exactly
607 which function of SMN is responsible for the phenotype observed in SMA patients. Likely, the
608 SMA phenotype could be due to a combination of different defects that would synergistically
609 impact cellular activities. Our results present here a newly discovered SMN function in
610 maintaining nucleolar homeostasis after DNA damage and repair. Importantly, we showed that
611 SMN-depleted cells show a moderate but remarkable sensitivity to UV-induced damage and
612 most importantly to chronic oxidative damage (Figure 8) which is what motoneurons would have
613 to deal with all along patients' life. This result is also important because they point to the fact that
614 not just the DNA repair process is important for cell viability but also all the processes that restore
615 cellular functions after DNA repair completion.
616 Our findings may directly impact the life and well-being of SMA patients [48]. In fact, in cells
617 and motoneurons of SMA patients, exogenous and endogenous DNA damage might
618 progressively and lastingly disrupt the nucleolar structure and disturb ribosome biogenesis
619 leading to perturbed protein translation [49]. This defect may contribute to the neurodegenerative
620 phenotype of SMA motoneurons. If this hypothesis is true, SMA patients could be advised to
621 prevent deleterious DNA damage to avoid a reorganization of the nucleolus that would affect
622 proper protein production within neurons. Although exogenous DNA damage is partially
623 avoidable, endogenous DNA damage is inevitable and one way to reduce its overload is to follow
624 a diet rich in antioxidants. This nutritional approach combined with a healthy lifestyle, avoiding
625 exogenous damage, such as cigarette smoke, pollutants, and potentially harmful molecules, may
626 retard the degeneration of motoneurons and thus SMA progression.
627
628
629

630 ## MATERIALS AND METHODS

631 ### Cells culture

632 SV40-immortalized human fibroblasts, wild-type (MRC5-SV) and CSB-deficient (CS1AN-
633 SV), were cultured in DMEM supplemented with 10% fetal bovine serum (FBS) and 1% penicillin
634 and streptomycin (P/S) and incubated at 37°C with 20% O2 and 5% CO2.

635 The MRC5-SV + Sh cells were obtained by transduction of lentiviral particles produced
636 (as described
637 https://www.addgene.org/protocols/plko/#Ehttps://www.addgene.org/protocols/plko/ - E) from
638 piSMART hEF1**α**/turboGFP (Dharmacon) doxycycline-inducible lentiviral system containing a
639 Short Hairpin (Sh) Scramble (VSC6572), Sh5-SMN (V3IHSHEG_4923340; mature antisense:
640 TAAACTACAACACCCTTCT) or Sh6-SMN (V3IHSHEG_5297527; mature antisense:
641 TTCAAATTTTCTCAACTGC). ShSMN both target telomeric *SMN1* and centromeric *SMN2* copies
642 of the gene. The cells were cultured in DMEM supplemented with 10% FBS and 1% P/S;
643 maintained in 100 ng/ml puromycin. Sh expression is induced with 100 ng/ml doxycycline. The
644 cells were incubated at 37°C with 20% O_2 and 5% CO_2.

645

646 ### Treatment

647 DNA damage was inflicted by UV-C light (254 nm, 6-Watt lamp). Cells were globally
648 irradiated with a UV-C dose of 16 J/m² or locally irradiated with a UV-C dose of 100 J/m² through
649 a filter with holes of 5µm. After irradiation, cells were incubated at 37°C with 5% CO2 for different
650 periods of time.

651 The PRMT inhibitor, MS023 (ab223596) diluted in DMSO, was added at 1µM in the
652 medium 20h before irradiation. The PRMT1 inhibitor, Furamidine (ab287098) diluted in DMSO,
653 was added at 1µM in the medium 15h before irradiation.

654 ### Transfection of small interfering RNAs (siRNAs)

655 Cells were seeded in six-well plates with coverslip and allowed to attach. Cells were
656 transfected two times in an interval of 24h with siRNA using Lipofectamine® RNAiMAX reagent
657 (Invitrogen; 13778150) according to the manufacturer' protocol. Experiments were performed

658 between 24h and 72h after the second transfection. Protein knock-down was confirmed for each
659 experiment by western blot. The small interfering RNA (siRNAs) used in this study are: siMock,
660 Horizon, D-001206-14 (10nM); siCOILIN, Horizon, M-019894-01 (5nM); siFBL, Horizon, L-011269-
661 00 (10nM); siPRMT1, Horizon, L-010102-00 (10nM). The final concentration used for each siRNA
662 is indicated in parentheses. All siRNA are a pool of four different siRNA.

663 **Protein extraction**

664 Cells were collected using trypsin or by scraping and centrifuged 10 min at 1400 rpm. To
665 verify siRNA efficiency, the coverslip need for the experiment was displaced before fixation and
666 cells that remained in the dish were collected. The extraction of total proteins was performed
667 using the PIERCE RIPA buffer (Thermo, #89900) complemented with EDTA-free cOmplete PIC
668 (ROCHE).

669 **Western blot**

670 Proteins were separated on a SDS-PAGE gel composed of bisacrylamide (37:5:1), and
671 then transferred onto a polyvinylidene difluoride membrane (PVDF, 0.45 µm; Millipore). The
672 membrane was blocked in PBS-T (PBS and 0.1 % Tween 20) with 5 % milk and incubated for 2h
673 at room temperature (RT) or overnight at 4°C with the primary antibodies diluted in milk PBS-T
674 (see table of antibody). Subsequently, the membrane was washed with PBS-T (3× 5-10 min) and
675 incubated with the following secondary antibody diluted 1/5000 in milk PBS-T: Goat anti-rabbit
676 IgG HRP conjugate (170-6515; BioRad) or Goat anti-mouse IgG HRP conjugate (170-6516;
677 BioRad). After the same washing procedure, protein bands were visualized via
678 chemiluminescence (ECL Enhanced Chemo Luminescence; Pierce ECL Western Blotting
679 Substrate) using the ChemiDoc MP system (BioRad).

680 **Cytostripping**

681 To improve the nuclear signal of immunofluorescence signal, the cytoplasm of the cells
682 was removed before fixation. After two washes with cold PBS, cells were incubated on ice 5 min
683 with cold cytoskeleton buffer (10mM PIPES pH6,8; 100mM NaCl; 300mM Sucrose; 3mM MgCl2;
684 1mM EGTA; 0,5% Triton-X100) followed by 5min with cold cytostripping buffer (10mM Tris HCL

685 pH7,4; 10mM NaCl; 3mM MgCl2; 1% Tween 40; 0,5% sodium deoxycholate). After three gentle
686 washes with cold PBS, cells were fixed.

687 Immunofluorescence

688 Cells were grown on coverslips, washed with PBS at RT, and fixed with 2%
689 paraformaldehyde (PFA) for 15min at 37° C. Cells were permeabilized with PBS 0.1 % Triton X-
690 100 (3X short + 2X 10 min washes). Blocking of non-specific signals was performed with PBS+
691 (PBS, 0.5 % BSA, 0.15 % glycine) for at least 30 min. Then, coverslips were incubated with primary
692 antibody diluted in PBS+ for 2h at room temperature (RT) or overnight at 4°C in a moist chamber.
693 After several washes with PBS + 0.1% Triton X-100 (3X short + 2X 10 min) and a quick washed
694 with PBS+, cells were incubated for 1h at RT in a moist chamber with the following secondary
695 antibody coupled to fluorochrome and diluted 1/400 in PBS+ : Goat anti-mouse Alexa Fluor®
696 488 [A11001, Invitrogen] or 594 [A11005] and Goat anti-rabbit Alexa Fluor® 488 [A11008] or 594
697 [A11012]. After the same washing procedure but with PBS, coverslips were finally mounted using
698 Vectashield with DAPI (Vector Laboratories).

699 Proximity ligation assay

700 PLA experiments were done using Duolink™ II secondary antibodies and detection kits
701 (Sigma-Aldrich, #DUO92002, #DUO92004, and #DUO92008) according to the manufacturer's
702 instructions. In brief, cells were fixed and permeabilized with the same procedure as
703 immunofluorescence followed by incubation in PLA blocking buffer for 1h at 37 °C. After
704 blocking, cells were incubated overnight at 4°C with primary antibodies diluted in PLA Antibody
705 Diluent. After washes with PLA buffer A (1 short + 3x5min), cells were incubated with PLUS and
706 MINUS PLA probes for 1h at 37 °C. After the same washing procedures with PLA buffer A, if
707 probes were in close proximity (<40 nm), they were ligated together to make a closed circle
708 thanks to the incubation of 30min at 37°C with the Duolink™ ligation solution. Then, after the
709 same washing procedures, the DNA is amplified and detected by fluorescence 594 thanks to the
710 incubation of 100min at 37°C with the Duolink™ amplification solution. After washing with PLA buffer
711 B (1 short + 2x10min), coverslips were mounted using Vectashield with DAPI (Vector Laboratories).

712 RNA Fluorescence In Situ Hybridization (RNA-FISH)

713 Cells were grown on coverslips and globally irradiated for different times. Then, cells were
714 washed with PBS at RT, and fixed with 4% PFA for 15min at 37° C. After two washes with PBS,
715 cells were permeabilized with PBS+ 0.4 % Triton X-100 for 7min at 4° C. Cells were washed
716 rapidly with PBS before incubation for at least 30min with pre-hybridization buffer (15%
717 formamide in 2X SSPE pH8.0 [0.3M NaCl, 15.7mM $NaH_2PO_4.H_2O$ and 2.5mM EDTA]). 35ng of
718 probe was diluted in 70µl of hybridization mix (2X SSPE, 15% formamide, 10% dextran sulfate
719 and 0.5mg/ml tRNA). Hybridization of the probe was conducted overnight at 37°C in a humidified
720 environment. Subsequently, cells were washed twice for 20 min with prehybridization buffer, then
721 once for 20 min with 1X SSPE. After extensive washing with PBS, the coverslips were mounted
722 with Vectashield containing DAPI (Vector Laboratories). The probe sequence (5' to 3') is Cy5-
723 AGACGAGAACGCCTGACACGCACGGCAC. At least 30 cells were imaged for each condition
724 of each cell lines.

725 **Primary Antibodies**

726 The following primary antibodies were used:

Antibody against	Manufacturer	Catalog Nr	Source	IF/PLA	WB
Alpha-Tubulin	Sigma	T6074	Mouse		1/50 000
Coilin	Proteintech	10967-1-AP	Rabbit	1/500	1/5000
CSB	Santa Cruz Biotechnology	sc398022	Mouse		1/100
FBL	Abcam	ab5821	Rabbit	1/500	1/500
GEMIN2	ABclonal	A3082	Rabbit	1/500	
GEMIN3	Santa Cruz Biotechnology	sc374373	Mouse	1/1000	
GEMIN4	Santa Cruz Biotechnology	sc365424	Mouse	1/1000	

GEMIN5	Proteintech	24897-1-AP	Rabbit	1/500	
PRMT1	Abcam	ab190892	Rabbit	1/5000	1/1000
RNAP1	Santa-cruz	sc48385	Mouse	1/500	
SMN	Proteintech	11708-1-AP	Rabbit	1/100	
SMN	BD Biosciences	610646	Mouse	1/500	1/5000

727

728 **Images acquisition and analysis and statistics**

729 Confocal images of the cells were obtained on a Zeiss LSM 880 NLO confocal laser
730 scanning inverted microscope using either a Plan-Apochromat 63x/1.4 or 40x/1.3 oil immersion
731 objective. Other images were obtained using an upright Zeiss Z1 Imager with a Plan-Apochromat
732 40x/0.95 objective. Time-lapse imaging of live cells for 48 hours was achieved on a Zeiss
733 AxioObserver 7 microscope with an Alpha Plan-Apochromat 63x/1.46 oil objective, equipped
734 with a dedicated incubator system set at 37°C and 5% CO_2.

735 Images of the cells for each experiment were obtained with the same microscopy system
736 and constant acquisition parameters. Images were analyzed with Image J software. For all images
737 of this study, nuclei and nucleoli were delimited with dashed and dotted lines respectively, using
738 DAPI staining.

739 Protein localization data represented as composite bar graphs was performed by manually
740 sorting cells based on protein localization. The number of cells analyzed per time point or
741 condition was between 100 and 300 cells, except for primary cells, motoneuons and GFP-SMN
742 expressing cells (50 to 100 cells).

743 All experiments have been performed at least three times (biological replicates). Error
744 bars represent the Standard Error of the Mean (SEM) of the biological replicates. Excel was used
745 for statistical analysis and plotting of all the numerical data. Statistics were performed using a
746 Student's test to compare two different conditions (siMock vs. siRNA X or No UV irradiation vs.
747 after irradiation) with the following parameters: two-tailed distribution and two-sample unequal
748 variance (heteroscedastic).

749

Acknowledgments

Dedicated to the mothers and fathers of children affected with SMA. We would like to thank Laura Trinkle-Mulcahy for the generous gift of the mCherry-N1. For access to the confocal microscope, we acknowledge the contribution of the imaging facility CIQLE (https://ciqle.univ-lyon1.fr - Centre d'imagerie Quantitative Lyon-Est - SFR Santé Lyon-Est (UAR3453 CNRS, US7 INSERM, UCBL), a member of LyMIC (Lyon Multiscale Imaging Center).

Conflicts of interest

The authors disclose no potential conflict of interest.

Funding

This work was supported by AFM-Téléthon (MyoNeurALP 1 and 2) and by Institut National du Cancer (InCa, PLBIO19-126).

SM was funded by Jazan university, Jazan, Saudi Arabia.

PL and OB are funded by an AFM-Téléthon grant (MyoNeurALP) and by the Joint Collaborative Research Program between the Centre for Neuromuscular Disease (University of Ottawa) and Institut NeuroMyoGène (INMG - Claude Bernard Université Lyon 1).

JC is funded by a Canadian Institutes of Health Research (CIHR) grant (MOP 123381) and CureSMA Canada.

773 **REFERENCES**

774 1. Dubois, M.-L. & Boisvert, F.-M. The Nucleolus: Structure and Function. in *The Functional*
775 *Nucleus* (eds. Bazett-Jones, D. P. & Dellaire, G.) 29–49 (Springer International Publishing, 2016).
776 doi:10.1007/978-3-319-38882-3_2.

777 2. Hernandez-Verdun, D. Assembly and disassembly of the nucleolus during the cell cycle.
778 *Nucl. Austin Tex* **2**, 189–194 (2011).

779 3. Boulon, S., Westman, B. J., Hutten, S., Boisvert, F.-M. & Lamond, A. I. The nucleolus
780 under stress. *Mol. Cell* **40**, 216–227 (2010).

781 4. Louvet, E., Junéra, H. R., Le Panse, S. & Hernandez-Verdun, D. Dynamics and
782 compartmentation of the nucleolar processing machinery. *Exp. Cell Res.* **304**, 457–470 (2005).

783 5. Giglia-Mari, G., Zotter, A. & Vermeulen, W. DNA damage response. *Cold Spring Harb.*
784 *Perspect. Biol.* **3**, a000745 (2011).

785 6. Brooks, P. J. The case for 8,5′-cyclopurine-2′-deoxynucleosides as endogenous DNA
786 lesions that cause neurodegeneration in xeroderma pigmentosum. *Neuroscience* **145**, 1407–
787 1417 (2007).

788 7. Kumar, N. *et al.* Global and transcription-coupled repair of 8-oxoG is initiated by
789 nucleotide excision repair proteins. *Nat. Commun.* **13**, 974 (2022).

790 8. Daniel, L. *et al.* Mechanistic insights in transcription-coupled nucleotide excision repair
791 of ribosomal DNA. *Proc. Natl. Acad. Sci. U. S. A.* **115**, E6770–E6779 (2018).

792 9. Cerutti, E. *et al.* **β**-Actin and Nuclear Myosin I are responsible for nucleolar
793 reorganization during DNA Repair. 646471 Preprint at https://doi.org/10.1101/646471 (2019).

794 10. Talbot, K. & Tizzano, E. F. The clinical landscape for SMA in a new therapeutic era. *Gene*
795 *Ther.* **24**, 529–533 (2017).

796 11. Monani, U. R. Spinal muscular atrophy: a deficiency in a ubiquitous protein; a motor
797 neuron-specific disease. *Neuron* **48**, 885–896 (2005).

798 12. Calucho, M. *et al.* Correlation between SMA type and SMN2 copy number revisited: An
799 analysis of 625 unrelated Spanish patients and a compilation of 2834 reported cases.
800 *Neuromuscul. Disord. NMD* **28**, 208–215 (2018).

801 13. Singh, R. N., Howell, M. D., Ottesen, E. W. & Singh, N. N. Diverse role of survival motor
802 neuron protein. *Biochim. Biophys. Acta Gene Regul. Mech.* **1860**, 299–315 (2017).

803 14. Trinkle-Mulcahy, L. & Sleeman, J. E. The Cajal body and the nucleolus: 'In a relationship'
804 or 'It's complicated'? *RNA Biol.* **14**, 739–751 (2017).

805 15. Hebert, M. D., Szymczyk, P. W., Shpargel, K. B. & Matera, A. G. Coilin forms the bridge
806 between Cajal bodies and SMN, the spinal muscular atrophy protein. *Genes Dev.* **15**, 2720–
807 2729 (2001).

808 16. Wehner, K. A. *et al.* Survival motor neuron protein in the nucleolus of mammalian
809 neurons. *Brain Res.* **945**, 160–173 (2002).

810 17. Jones, K. W. *et al.* Direct interaction of the spinal muscular atrophy disease protein SMN
811 with the small nucleolar RNA-associated protein fibrillarin. *J. Biol. Chem.* **276**, 38645–38651
812 (2001).

813 18. Renvoisé, B. *et al.* Distinct domains of the spinal muscular atrophy protein SMN are
814 required for targeting to Cajal bodies in mammalian cells. *J. Cell Sci.* **119**, 680–692 (2006).

815 19. Thandapani, P., O'Connor, T. R., Bailey, T. L. & Richard, S. Defining the RGG/RG motif.
816 *Mol. Cell* **50**, 613–623 (2013).

817 20. Jacquier, A. *et al.* Severe congenital myasthenic syndromes caused by agrin mutations
818 affecting secretion by motoneurons. *Acta Neuropathol. (Berl.)* **144**, 707–731 (2022).

819 21. Pellizzoni, L., Baccon, J., Charroux, B. & Dreyfuss, G. The survival of motor neurons
820 (SMN) protein interacts with the snoRNP proteins fibrillarin and GAR1. *Curr. Biol. CB* **11**, 1079–
821 1088 (2001).

822 22. Whitehead, S. E. *et al.* Determinants of the Interaction of the Spinal Muscular Atrophy
823 Disease Protein SMN with the Dimethylarginine-modified Box H/ACA Small Nucleolar
824 Ribonucleoprotein GAR1 *. *J. Biol. Chem.* **277**, 48087–48093 (2002).

825 23. Cioce, M., Boulon, S., Matera, A. G. & Lamond, A. I. UV-induced fragmentation of Cajal
826 bodies. *J. Cell Biol.* **175**, 401–413 (2006).

827 24. Kawanishi, S. & Murata, M. Mechanism of DNA damage induced by bromate differs
828 from general types of oxidative stress. *Toxicology* **221**, 172–178 (2006).

829 25. Tessarz, P. *et al.* Glutamine methylation in histone H2A is an RNA-polymerase-I-
830 dedicated modification. *Nature* **505**, 564–568 (2014).

831 26. Gupta, K. *et al.* Assembly of higher-order SMN oligomers is essential for metazoan
832 viability and requires an exposed structural motif present in the YG zipper dimer. *Nucleic Acids*
833 *Res.* **49**, 7644–7664 (2021).

834 27. Friesen, W. J., Massenet, S., Paushkin, S., Wyce, A. & Dreyfuss, G. SMN, the product of
835 the spinal muscular atrophy gene, binds preferentially to dimethylarginine-containing protein
836 targets. *Mol. Cell* **7**, 1111–1117 (2001).

837 28. Sprangers, R., Groves, M. R., Sinning, I. & Sattler, M. High-resolution X-ray and NMR

838 structures of the SMN Tudor domain: conformational variation in the binding site for
839 symmetrically dimethylated arginine residues. *J. Mol. Biol.* **327**, 507–520 (2003).

840 29. Fulton, M. D., Brown, T. & Zheng, Y. G. Mechanisms and Inhibitors of Histone Arginine
841 Methylation. *Chem. Rec. N. Y. N* **18**, 1792–1807 (2018).

842 30. Bedford, M. T. & Richard, S. Arginine methylation an emerging regulator of protein
843 function. *Mol. Cell* **18**, 263–272 (2005).

844 31. Di Lorenzo, A. & Bedford, M. T. Histone arginine methylation. *FEBS Lett.* **585**, 2024–
845 2031 (2011).

846 32. Lee, Y.-H. & Stallcup, M. R. Minireview: protein arginine methylation of nonhistone
847 proteins in transcriptional regulation. *Mol. Endocrinol. Baltim. Md* **23**, 425–433 (2009).

848 33. Hebert, M. D., Shpargel, K. B., Ospina, J. K., Tucker, K. E. & Matera, A. G. Coilin
849 methylation regulates nuclear body formation. *Dev. Cell* **3**, 329–337 (2002).

850 34. Eram, M. S. *et al.* A Potent, Selective, and Cell-Active Inhibitor of Human Type I Protein
851 Arginine Methyltransferases. *ACS Chem. Biol.* **11**, 772–781 (2016).

852 35. Yan, L. *et al.* Diamidine compounds for selective inhibition of protein arginine
853 methyltransferase 1. *J. Med. Chem.* **57**, 2611–2622 (2014).

854 36. Prusty, A. B. *et al.* Impaired spliceosomal UsnRNP assembly leads to Sm mRNA down-
855 regulation and Sm protein degradation. *J. Cell Biol.* **216**, 2391–2407 (2017).

856 37. Stuart, J. A. *et al.* How Supraphysiological Oxygen Levels in Standard Cell Culture Affect
857 Oxygen-Consuming Reactions. *Oxid. Med. Cell. Longev.* **2018**, 1–13 (2018).

858 38. Otter, S. *et al.* A Comprehensive Interaction Map of the Human Survival of Motor
859 Neuron (SMN) Complex. *J. Biol. Chem.* **282**, 5825–5833 (2007).

860 39. Pellizzoni, L., Yong, J. & Dreyfuss, G. Essential Role for the SMN Complex in the
861 Specificity of snRNP Assembly. *Science* **298**, 1775–1779 (2002).

862 40. Zhao, D. Y. *et al.* SMN and symmetric arginine dimethylation of RNA polymerase II C-
863 terminal domain control termination. *Nature* **529**, 48–53 (2016).

864 41. Tisdale, S. *et al.* SMN is essential for the biogenesis of U7 small nuclear
865 ribonucleoprotein and 3'-end formation of histone mRNAs. *Cell Rep.* **5**, 1187–1195 (2013).

866 42. Fallini, C., Donlin-Asp, P. G., Rouanet, J. P., Bassell, G. J. & Rossoll, W. Deficiency of the
867 Survival of Motor Neuron Protein Impairs mRNA Localization and Local Translation in the
868 Growth Cone of Motor Neurons. *J. Neurosci. Off. J. Soc. Neurosci.* **36**, 3811–3820 (2016).

869 43. Sanchez, G. *et al.* A novel function for the survival motoneuron protein as a translational

870 regulator. *Hum. Mol. Genet.* **22**, 668–684 (2013).

871 44. Cauchi, R. J. SMN and Gemins: 'We are family' … or are we?: Insights into the
872 partnership between Gemins and the spinal muscular atrophy disease protein SMN. *BioEssays*
873 **32**, 1077–1089 (2010).

874 45. Martinez-Salas, E., Embarc-Buh, A. & Francisco-Velilla, R. Emerging Roles of Gemin5:
875 From snRNPs Assembly to Translation Control. *Int. J. Mol. Sci.* **21**, 3868 (2020).

876 46. Meister, G. *et al.* Methylation of Sm proteins by a complex containing PRMT5 and the
877 putative U snRNP assembly factor pICln. *Curr. Biol. CB* **11**, 1990–1994 (2001).

878 47. Lin, C.-H., Huang, H.-M., Hsieh, M., Pollard, K. M. & Li, C. Arginine methylation of
879 recombinant murine fibrillarin by protein arginine methyltransferase. *J. Protein Chem.* **21**, 447–
880 453 (2002).

881 48. Lomonte, P., Baklouti, F. & Binda, O. The Biochemistry of Survival Motor Neuron Protein
882 Is Paving the Way to Novel Therapies for Spinal Muscle Atrophy. *Biochemistry* **59**, 1391–1397
883 (2020).

884 49. Karyka, E. *et al.* SMN-deficient cells exhibit increased ribosomal DNA damage. *Life Sci.*
885 *Alliance* **5**, e202101145 (2022).

886